

Revisiting Connes' Finite Spectral Distance on Non-commutative Spaces : Moyal Plane and Fuzzy Sphere

Yendrembam Chaoba Devi*, Alpesh Patil†, Aritra N Bose*,
Kaushlendra Kumar‡, Biswajit Chakraborty*, Frederik G Scholtz§

November 5, 2018

Abstract

We revise and extend the algorithm provided in [1] to compute the finite Connes' distance between normal states. The original formula in [1] contains an error and actually only provides a lower bound. The correct expression, which we provide here, involves the computation of the infimum of an expression which involves the “transverse” component of the algebra element in addition to the “longitudinal” component of [1]. This renders the formula less user-friendly, as the determination of the exact transverse component for which the infimum is reached remains a non-trivial task, but under rather generic conditions it turns out that the Connes' distance is proportional to the trace norm of the difference in the density matrices, leading to considerable simplification. In addition, we can determine an upper bound of the distance by emulating and adapting the approach of [2] in our Hilbert-Schmidt operatorial formulation. We then look for an optimal element for which the upper bound is reached. We are able to find one for the Moyal plane through the limit of a sequence obtained by finite dimensional projections of the representative of an element belonging to a multiplier algebra, onto the subspaces of the total Hilbert space, occurring in the spectral triple and spanned by the eigen-spinors of the respective Dirac operator. This is in contrast with the fuzzy sphere, where the upper bound, which is given by the geodesic of a commutative sphere is never reached for any finite n -representation of $SU(2)$. Indeed, for the case of maximal non-commutativity ($n = 1/2$), the finite distance is shown to coincide exactly with the above mentioned lower bound, with the transverse component playing no role. This, however starts changing from $n = 1$ onwards and we try to improve the estimate of the finite distance and provide an almost exact result, using our new and modified algorithm.

1 Introduction

It is quite plausible that the structure of space-time in the vicinity of Planck scale is described by a fuzzy “quantum space-time”. As shown by Doplicher *et. al* [3], this quantum structure of space-time, where the space-time coordinates are operator-valued and satisfy a non-commuting coordinate algebra, can be one of the most plausible ways to prevent the gravitational collapse arising from the attempt to localise a space-time event within a Planck length scale. Since making a guess regarding the non-commutative structure of the coordinate algebra is difficult, one tries to postulate a simple structure of this form and study the geometry of the resulting non-commutative spaces. The simplest examples are the 2D Moyal plane (\mathbb{R}_*^2):

$$[\hat{x}_1, \hat{x}_2] = i\theta, \quad (1)$$

and fuzzy \mathbb{R}_*^3 :

$$[\hat{x}_i, \hat{x}_j] = i\lambda\epsilon_{ijk}\hat{x}_k. \quad (2)$$

Fuzzy sphere \mathbb{S}_*^2 corresponds to a 2D subspace of \mathbb{R}_*^3 with radius quantized as $r_n = \lambda\sqrt{n(n+1)}$ [4]. Because of the inherent uncertainty relations satisfied by these coordinates the usual concepts like points, lines etc lose their meaning in these kinds of spaces. It thus becomes essential to use the mathematical formalism of Non-Commutative Geometry(NCG) as developed by Connes [5] to study the geometry of such spaces.

We would like to mention in this context that Connes himself, along with his other collaborators, have invested a lot of effort in formulating a completely new mathematical framework to describe the Standard model of particle physics, by invoking the so-called “Almost Commutative Spaces” - built out of the usual commutative (Euclideanised) 4D curved space-time. This is expected to describe physics upto GUT scale ($\sim 10^{15} GeV$). However, as we mentioned in the beginning, one perhaps has to take quantum space-times, i.e. spaces where the coordinates become operators satisfying a non-commutative algebra and for which (1) and (2) provide prototype examples, more seriously in the

*S.N.Bose National Centre For Basic Sciences, Salt Lake, Kolkata 700098, India; Email: chaoba@bose.res.in, anb@bose.res.in, biswajit@bose.res.in

†Indian Institute of Science Education and Research(IISER), Pune 411008, India ; Email: alpeshp93@gmail.com

‡Indian Institute of Science Education and Research(IISER) Kolkata, Nadia 741 252 WB, India; Email: kk15ip019@iiserkol.ac.in

§National Institute for Theoretical Physics (NITheP), Stellenbosch 7602, South Africa; Email: fgs@sun.ac.za

higher energy scales - like in the vicinity of Planck scales. (See for example [6] for a review). It is only recently that the above mentioned mathematical framework of NCG, *a la* Connes, has been used to compute the spectral distances on “quantized spaces” like the Moyal plane, fuzzy sphere etc. [2],[7]-[12]. On the other hand, an algorithm was devised in [1] to compute this distance using the Hilbert-Schmidt operatorial formulation of quantum mechanics [13], [14]. This Hilbert-Schmidt operatorial formulation has the advantage that it bypasses the use of any star product, like Moyal or Voros, and is therefore free from any ambiguities that can arise from there [15]. Furthermore, it has an additional advantage that the above-mentioned algorithm/formula is adaptable to this Hilbert-Schmidt operatorial formulation and infinitesimally it has essentially the same structure as that of the induced metric from the Hilbert space inner product, obtained by Provost and Vallee [16] (See also [17]), when expressed in terms of the density matrix [1] and yields for the Moyal plane the correct distance in the “harmonic oscillator basis” and the flat metric in the coherent state, upto an overall numerical factor. However, the corresponding finite distance can not simply be obtained just by “integrating” along the geodesics, as the very concept of geodesics in the conventional sense (i.e. like on a commutative differentiable manifold) may not exist at all. This motivates us to undertake the task of extending our algorithm of [1] so that one is able to compute finite distances as well. This new formula is shown to involve the ‘transverse’ component ($\Delta\rho_{\perp}$), in addition to the “longitudinal” component ($\Delta\rho_{\parallel} \equiv \Delta\rho$) where $\Delta\rho$ is the difference between normal states represented by density matrices, as in [1]. This in turn shows that the formula of [1] actually corresponds only to the lower bound of the distance and not the actual distance. Indeed, on the way to our derivation of the generalised formula in section 3 we point out a flaw, commented on in [18] through a counter example, in the analysis in [1] where the same expression was shown to correspond to the upper bound as well. It should, however, be mentioned that the counter example in [18] does not satisfy the boundedness condition imposed in [1]. This error was not serious in examples studied previously to compute infinitesimal distances as these distances coincided with the exact distance for discrete states and differed from the exact distance by a numerical factor for the coherent states for both \mathbb{R}_*^2 and \mathbb{S}_*^2 [1, 4]. However, as one can easily see, a straightforward calculation to compute *finite* distances, using the same formula does not yield any sensible result indicating a non-trivial role for the transverse component $\Delta\rho_{\perp}$. In the generic case there can be many choices of $\Delta\rho_{\perp}$ to a given $\Delta\rho$ (in fact an infinite number of them in \mathbb{R}_*^2). Consequently the computation of the infimum involving $\Delta\rho_{\perp}$ occurring in the revised formula turns out to be quite non-trivial. One therefore has to try with different forms of $\Delta\rho_{\perp}$ and improve the estimate of the distance as best as one can.

On the other hand, we can emulate and adapt the approach of [2] to our Hilbert-Schmidt operatorial formulation to obtain an upper bound to the distance and then look for an optimal element in the algebra saturating this upper bound. In case at least one such optimal element can be identified, this upper bound itself can obviously be recognised as the true distance. Otherwise one has to be content with the above-mentioned best possible estimate only. In fact this paper deals with an interplay of both the approaches, as they seem to complement each other in some sense. This brings out some stark differences between \mathbb{R}_*^2 and \mathbb{S}_*^2 . Particularly for \mathbb{S}_*^2 corresponding to any finite n -representation of $SU(2)$ one can not define a geodesic in the conventional sense; it reduces to commutative \mathbb{S}^2 only in the limit $n \rightarrow \infty$. The distance turns out to be much smaller than the geodesic distance of \mathbb{S}^2 , the latter coinciding with the above-mentioned upper bound. Further in the case of maximal non-commutativity i.e. for $n = 1/2$, even the finite distance is shown to coincide exactly with the lower bound with $\Delta\rho_{\perp}$ playing no role and any pair of pure states is shown to be interpolated by a one-parameter family of mixed states, lying in the interior of \mathbb{S}_*^2 . The distance between any mixed state to the nearest pure state can be taken as a measure of the ‘mixedness’.

The whole analysis, particularly the “ball condition” is carried out in the eigen-spinor basis furnished by the respective Dirac operators. This is clearly a natural choice of basis, as the ball condition involves the Dirac operator. This definitely simplifies the computations considerably and even allows us to study the geometry of \mathbb{S}_*^2 for $n = 1$, apart from reproducing many of the existing results in the literature, albeit with the help of *Mathematica*. However the corresponding analysis for $n > 1$ remains quite intractable, even with *Mathematica*.

The paper is organised as follows. In section 2, we provide a brief review of the Hilbert-Schmidt operatorial formulation of non-commutative quantum mechanics on the 2D-Moyal plane and fuzzy sphere and the associated spectral triples, introduced in [1, 4] - required to study the geometrical aspects of them. We also introduce the corresponding Dirac operators and their eigen-spinors for both non-commutative spaces. To begin, we revisit the derivation of the formula given in [1] in section 3 and derive the corrected form. We then provide a computation of (finite) distances on the Moyal plane in the coherent and the “harmonic oscillator” basis in sections 4 and 5, respectively. We then proceed onto the case of the fuzzy sphere in quite the same way adopted as in the Moyal plane in section 6. We note some fundamental differences from the case of the Moyal plane and adopt a different algorithm using the Dirac eigen-spinors and study the $n = 1/2$ and $n = 1$ representations of the fuzzy sphere algebra. We finally conclude in section 7.

2 Review of Hilbert-Schmidt operatorial formulation and the spectral triples for non-commutative spaces (\mathbb{R}_*^2 and \mathbb{S}_*^2)

2.1 Moyal Plane (\mathbb{R}_*^2)

The Hilbert-Schmidt operatorial formulation of Non-Commutative Quantum Mechanics (NCQM) on the 2D Moyal plane [13, 14], described by the non-commutative Heisenberg algebra i.e. the co-ordinate algebra (1) augmented by the following commutation relations involving linear momenta operators \hat{p}_i satisfying (in units of $\hbar = 1$)

$$[\hat{x}_i, \hat{p}_j] = i\delta_{ij} \quad ; \quad [\hat{p}_i, \hat{p}_j] = 0 \quad (3)$$

begins by introducing an auxiliary Hilbert space \mathcal{H}_c furnishing a representation of just the coordinate algebra (1). In this particular situation, since the algebra (1) is isomorphic to the algebra $[\hat{x}, \hat{p}] = i$ of a 1D harmonic oscillator, \mathcal{H}_c can be constructed exactly in the same manner i.e.

$$\mathcal{H}_c = \text{Span} \left\{ |n\rangle = \frac{(b^\dagger)^n}{\sqrt{n!}} |0\rangle \right\}_{n=0}^{\infty} \quad (4)$$

where $b = \frac{1}{\sqrt{2\theta}}(\hat{x}_1 + i\hat{x}_2)$ and b^\dagger are the respective lowering and raising operators satisfying $[b, b^\dagger] = 1$ and the "ground state" $|0\rangle$ satisfy $b|0\rangle = 0$. This \mathcal{H}_c , however, cannot furnish a representation of the linear momentum operators \hat{p}_i . As shown in [13, 14], we need to introduce the space \mathcal{H}_q comprised of Hilbert-Schmidt operators acting on \mathcal{H}_c . Loosely speaking, these are essentially the trace-class bounded set of operators and forms a Hilbert space on its own referred to as the quantum Hilbert space. Physical states $|\psi\rangle$ (denoted by round kets, rather than angular kets $|\cdot\rangle \in \mathcal{H}_c$ (4)), having generic forms as

$$|\psi\rangle = \sum_{m,n} \psi_{m,n} |m\rangle \langle n| \in \mathcal{H}_q \quad (5)$$

and the inner product between a pair of such states $|\psi\rangle, |\phi\rangle \in \mathcal{H}_q$ is defined as

$$(\phi|\psi) = \text{tr}_c(\phi^\dagger \psi) \quad (6)$$

where the subscript \mathcal{H}_c in (6) indicates that the trace has to be computed over \mathcal{H}_c .

We reserve \dagger to denote the hermitian conjugation on \mathcal{H}_c (4), while \ddagger denotes the hermitian conjugation on \mathcal{H}_q . Note that \mathcal{H}_q has a natural tensor product structure as $\mathcal{H}_q = \mathcal{H}_c \otimes \mathcal{H}_c^*$ (\mathcal{H}_c^* being the dual of \mathcal{H}_c), enabling one to express the elements of \mathcal{H}_q in the form $|\psi, \phi\rangle = |\psi\rangle \langle \phi|$ or their linear spans. One can refer to ψ (respectively ϕ) as the left (respectively right) hand sector.

A unitary representation of the non-commutative Heisenberg algebra (1) and (3) is obtained by the following actions:

$$\hat{X}_i |\psi\rangle = |\hat{x}_i \psi\rangle \quad ; \quad \hat{P}_i |\psi\rangle = \frac{1}{\theta} \epsilon_{ij} |\hat{x}_j, \psi\rangle. \quad (7)$$

Note that we are using capital letters (without hats) to distinguish them from the operators acting on \mathcal{H}_c . Apart from the "harmonic oscillator" basis $|n\rangle$, introduced in (4), satisfying $b^\dagger b |n\rangle = n |n\rangle$, one can also introduce normalized coherent states in terms of a dimensionless complex number $z = \frac{1}{\sqrt{2\theta}}(x_1 + ix_2)$ as

$$|z\rangle = U(z, \bar{z}) |0\rangle \quad ; \quad U(z, \bar{z}) = e^{-\bar{z}b + zb^\dagger}, \quad (8)$$

where $U(z, \bar{z})$ is a unitary operator furnishing a projective representation of the translation group. These states provide an over-complete basis in \mathcal{H}_c . The corresponding non-orthogonal projection operator $\rho_z \equiv |z\rangle \langle z| \equiv |z\rangle \in \mathcal{H}_q$ is an operator acting on \mathcal{H}_c and is an eigenstate of B (the representation of \hat{b} in \mathcal{H}_q) : $B|z\rangle = z|z\rangle$. This represents a quantum state with maximal localization, where the position measure must now be interpreted in the context of a weak measurement (Positive Operator-Valued Measurement, POVM) rather than a strong measurement (Projective Valued Measurement, PVM). As was shown in [19] this quantum Hilbert space \mathcal{H}_q has a built-in structure of an algebra in the sense that under the multiplication map 'm' the usual operator product of any arbitrary pair of elements $|\phi\rangle, |\psi\rangle \in \mathcal{H}_q$ yields another element of \mathcal{H}_q :

$$\begin{aligned} m : \mathcal{H}_q \otimes \mathcal{H}_q &\rightarrow \mathcal{H}_q, \\ |\phi\rangle \otimes |\psi\rangle &\rightarrow |\phi\psi\rangle. \end{aligned} \quad (9)$$

It was further shown in [19] that the representation i.e. the symbols of the above composite state $|\phi\psi\rangle$ in the coherent state i.e. $(z|\phi\psi)$ is obtained by composing the respective representations of individual states i.e. $(z|\phi)$ and $(z|\psi)$ by using the Voros star product $*_V$:

$$(z|\phi\psi) = 4\pi^2(z|\phi) *_V (z|\psi) \ ; \quad *_V = e^{\overleftarrow{\partial_z}\overrightarrow{\partial_z}}. \quad (10)$$

Furthermore, it was shown in [14] that $|z\rangle \in \mathcal{H}_q$ also provides an over-complete basis on \mathcal{H}_q - the counterpart of $|z\rangle \in \mathcal{H}_c$, provided that they are composed using the above mentioned Voros star product (10) :

$$\mathbb{1}_q = \int \frac{dzd\bar{z}}{\pi} |z\rangle *_V \langle z|. \quad (11)$$

Correspondingly, one can introduce the unnormalized projection operators

$$\pi_z = \frac{1}{2\pi\theta} |z\rangle *_V \langle z| \ ; \quad \pi_z^2 \propto \pi_z, \quad (12)$$

which are positive (i.e. $(\psi|\pi_z|\psi) \geq 0 \ \forall \ |\psi\rangle \in \mathcal{H}_q$) but unnormalized ($\pi_z^2 \propto \pi_z$) and non-orthogonal. They, however, form a complete basis and therefore provide a POVM (Positive Operator Valued Measure) that one can use to provide a consistent probability interpretation by assigning the probability density

$$P(x_1, x_2) = \text{tr}_q(\pi_z \Omega) \quad (13)$$

of finding the outcome of a position measurement to be (x_1, x_2) if the system is in a state described by the density matrix Ω . In particular, if $\Omega = |\psi\rangle\langle\psi|$ is a pure state density matrix, then

$$P(x_1, x_2) = \text{tr}_q(\pi_z \Omega) = (\psi|\pi_z|\psi) = \frac{1}{2\pi\theta} (\psi|z\rangle *_V \langle z|\psi), \quad (14)$$

which clearly goes into the corresponding commutative result in the limit $\theta \rightarrow 0$.

We briefly mention in this context that, just as the basis $|z\rangle \in \mathcal{H}_q$ has a natural association with the Voros star product (10), it was shown in [19] that one can like-wise construct an appropriate basis, which is naturally associated with the Moyal star product $*_M = e^{\frac{i}{2}\theta\epsilon_{ij}\overleftarrow{\partial_i}\overrightarrow{\partial_j}}$ (in the Cartesian $x_1 - x_2$ basis). However, this basis is somewhat unphysical in the sense that it is the common eigenstate of mathematically constructed unphysical commuting position-like observables \hat{X}_i^C , obtained by taking the average of left and right actions of \hat{X}_i as $\hat{X}_i^C = \frac{1}{2}(\hat{X}_i^L + \hat{X}_i^R)$ satisfying $[\hat{X}_i^C, \hat{X}_j^C] = 0$. Furthermore, they do not conform to the requirement of a POVM, unlike the Voros case discussed above. Besides, the representation of the quantum states in this Moyal basis lead to a different class of functions than the corresponding Voros ones. This implies that the equivalence between different choices of star products cannot be guaranteed, especially in a path integral formulations, without taking due care of this point.

2.2 Fuzzy Sphere (\mathbb{S}_*^2)

Here, the position operators satisfy the $su(2)$ commutation relation (2). This can be realized through a pair of oscillators using the Jordan-Schwinger map:

$$\hat{x}_i = \hat{\chi}^\dagger \sigma_i \hat{\chi} = \hat{\chi}_\alpha^\dagger \sigma_i^{\alpha\beta} \hat{\chi}_\beta, \quad \text{where } \sigma_i \text{ are the Pauli matrices.} \quad (15)$$

Here, $\hat{\chi}_\alpha/\hat{\chi}_\alpha^\dagger$ satisfy the following commutation relations:

$$[\hat{\chi}_\alpha, \hat{\chi}_\beta^\dagger] = \frac{1}{2}\lambda\delta_{\alpha\beta}, \quad [\hat{\chi}_\alpha, \hat{\chi}_\beta] = 0 = [\hat{\chi}_\alpha^\dagger, \hat{\chi}_\beta^\dagger]; \quad \alpha, \beta = 1, 2. \quad (16)$$

Common eigenstates of \hat{x}^2 and \hat{x}_3 can be constructed as follows:

$$|n, n_3\rangle = \sqrt{\frac{(2/\lambda)^{2n}}{(n+n_3)!(n-n_3)!}} \chi_1^{\dagger(n+n_3)} \chi_2^{\dagger(n-n_3)} |0\rangle, \quad (17)$$

with eigenvalues $r_n^2 = \lambda n(n+1)$ and $x_3 = \lambda n_3$, respectively. We define the ladder operators $\hat{x}_\pm = \hat{x}_1 \pm i\hat{x}_2$ which satisfy the commutation relations:

$$[\hat{x}_3, \hat{x}_\pm] = \pm\lambda\hat{x}_\pm; \quad [\hat{x}_+, \hat{x}_-] = 2\lambda\hat{x}_3. \quad (18)$$

Hence the classical configuration space \mathcal{F}_c of a fuzzy space of type (2) is given by

$$\mathcal{F}_c = \text{Span}\{|n, n_3\rangle \mid \forall n \in \mathbb{Z}/2, \ -n \leq n_3 \leq n\}. \quad (19)$$

Each n corresponds to the fixed sphere of radius $r_n = \lambda\sqrt{n(n+1)}$ such that for a fixed n the corresponding Hilbert sub-space is a $(2n+1)$ -dimensional sub-space

$$\mathcal{F}_n = \text{Span}\{|n, n_3\rangle \mid n \text{ is fixed}, \ -n \leq n_3 \leq n\}. \quad (20)$$

However, since the quantum Hilbert space, in which the physical states are represented, consists of those operators generated by coordinate operators only and since these commute with the Casimir the elements of the quantum Hilbert

space must in addition commute with the Casimir, i.e., must be diagonal in n . Therefore, the quantum Hilbert space \mathcal{H}_q of the fuzzy space of type (2) splits into the direct sum of sub-spaces as follows:

$$\mathcal{H}_q = \{\Psi \in \text{Span}\{|n, n_3\rangle\langle n, n'_3|\} : \text{tr}_c(\Psi^\dagger \Psi) < \infty\} = \bigoplus_n \mathcal{H}_n, \quad (21)$$

where

$$\mathcal{H}_n = \{\Psi \in \text{Span}\{|n, n_3\rangle\langle n, n_3|\} \equiv |n_3, n'_3\rangle : \text{tr}_c(\Psi^\dagger \Psi) < \infty \text{ with fixed } n\}, \quad (22)$$

represents the quantum Hilbert space of a fuzzy sphere with fixed radius $r_n = \lambda\sqrt{n(n+1)}$.

2.2.1 Perelomov's $SU(2)$ coherent states

The coherent states are the quantum states which saturate the Heisenberg's uncertainty relation. Each coherent state $|z\rangle$ is obtained by the action of a unitary operator $U(z)$ on the highest weight state $|n, n\rangle$, satisfying $\hat{x}_+|n, n\rangle = 0$, and is specified by a complex number z . It is well-known that $\| |z\rangle - |z'\rangle \| \rightarrow 0$ as $|z - z'| \rightarrow 0$ and hence implies that coherent states have the properties of classical states.

Here we review the construction of generalized coherent states of the $SU(2)$ group [10] such that the non-commutative analog of the homogeneous space of the fuzzy sphere can be constructed by using the Perelomov's $SU(2)$ coherent states [11]. Note that the Heisenberg uncertainty relations for the fuzzy sphere is given by

$$\Delta\hat{x}_1\Delta\hat{x}_2 \geq \frac{\lambda}{2}|\langle\hat{x}_3\rangle| \implies \Delta\hat{x}_1\Delta\hat{x}_2 = \frac{\lambda}{2}|\langle\hat{x}_3\rangle| = \frac{1}{2}\lambda^2n \quad (23)$$

for both bases build on $|n, n\rangle$ and $|n, -n\rangle$. Thus, we can choose the highest weight state as $|n, n\rangle$ and the Perelomov $SU(2)$ coherent states can be obtained by the action of a representation $T(g)$ of $g \in SU(2)$ on $|n, n\rangle$. Note that any action of \hat{x}_3 on the state $|n, n\rangle$ does not change it so that the group element generated by \hat{x}_3 is the stability subgroup of $SU(2)$. This implies that the set of generalized coherent states of $SU(2)$ is topologically isomorphic to the coset space $SU(2)/U(1) \simeq \mathbb{S}^2$. However, geometrically it reduces to \mathbb{S}^2 only in the limit $n \rightarrow \infty$.

We know that the operator $T(g)$, $\forall g \in SU(2)$ can be expressed in terms of Euler angles as $T(g) = e^{-i\frac{\varphi}{\lambda}\hat{x}_3} e^{-i\frac{\theta}{\lambda}\hat{x}_2} e^{-i\frac{\psi}{\lambda}\hat{x}_3}$ [10]. For \mathbb{S}^2 , $\psi = 0$ such that a generic coherent state specified by a point on \mathbb{S}^2 is given by

$$|z\rangle = e^{-i\frac{\varphi}{\lambda}\hat{x}_3} e^{-i\frac{\theta}{\lambda}\hat{x}_2} |n, n\rangle \xrightarrow{\varphi=0} e^{-i\frac{\theta}{\lambda}\hat{x}_2} |n, n\rangle = e^{\frac{\theta}{2\lambda}(\hat{x}_- - \hat{x}_+)} |n, n\rangle. \quad (24)$$

Here, z is the stereographic variable of \mathbb{S}^2 projected from the south pole to the complex plane $z = 1$ and $z = -\tan\frac{\theta}{2}e^{i\varphi}$.

2.3 Spectral Triple : Moyal Plane

The basic ingredients of studying the geometrical content, particularly Connes' distance on \mathcal{H}_c is facilitated by specifying the spectral triple $(\mathcal{A}, \mathcal{H}, \mathcal{D})$ where the algebra \mathcal{A} is identified with \mathcal{H}_q as mentioned above (9) and the Hilbert space \mathcal{H} is the module and identified with $\mathcal{H}_c \otimes \mathbb{C}^2$ so that it represents the space of appropriate "spinors" where a typical element $a \in \mathcal{A} = \mathcal{H}_q$ acts on $\Psi = \begin{pmatrix} |\psi_1\rangle \\ |\psi_2\rangle \end{pmatrix}$ through the diagonal representation π as

$$\pi(a)\Psi = \pi(a) \begin{pmatrix} |\psi_1\rangle \\ |\psi_2\rangle \end{pmatrix} = \begin{pmatrix} a & 0 \\ 0 & a \end{pmatrix} \begin{pmatrix} |\psi_1\rangle \\ |\psi_2\rangle \end{pmatrix} = \begin{pmatrix} a|\psi_1\rangle \\ a|\psi_2\rangle \end{pmatrix}. \quad (25)$$

The Dirac operator, as explained in detail in [4] (see also the Appendix A), is identified as

$$\mathcal{D} = \sqrt{\frac{2}{\theta}} \begin{pmatrix} 0 & b^\dagger \\ b & 0 \end{pmatrix}, \quad (26)$$

having a well-defined left action on $\mathcal{H}_c \otimes \mathbb{C}^2$ as

$$\mathcal{D}\Psi = \sqrt{\frac{2}{\theta}} \begin{pmatrix} 0 & b^\dagger \\ b & 0 \end{pmatrix} \begin{pmatrix} |\psi_1\rangle \\ |\psi_2\rangle \end{pmatrix} = \sqrt{\frac{2}{\theta}} \begin{pmatrix} b^\dagger|\psi_2\rangle \\ b|\psi_1\rangle \end{pmatrix}. \quad (27)$$

The eigen-spinors of the Dirac operator for the Moyal plane are given by the following,

$$|0\rangle := \begin{pmatrix} |0\rangle \\ 0 \end{pmatrix} \in \mathcal{H}_c \otimes \mathbb{C}^2 ; \quad |m\rangle_\pm := \frac{1}{\sqrt{2}} \begin{pmatrix} |m\rangle \\ \pm|m-1\rangle \end{pmatrix} \in \mathcal{H}_c \otimes \mathbb{C}^2 ; \quad m = 1, 2, 3, \dots \quad (28)$$

with the eigenvalues λ_m for any state $|m\rangle_\pm$ given by

$$\lambda_0 = 0 \quad ; \quad \lambda_m^\pm = \pm\sqrt{\frac{2m}{\theta}}.$$

They furnish a complete and orthonormal basis for $\mathcal{H}_c \otimes \mathbb{C}^2$, so that the resolution of the identity takes the form

$$\mathbf{1}_{\mathcal{H}_q \otimes M_2(\mathbb{C})} = |0\rangle\langle 0| + \sum_{m=1}^{\infty} \left(|m\rangle_+ \langle m| + |m\rangle_- \langle m| \right); \quad \pm \langle m|n\rangle_\pm = \delta_{mn}; \quad \pm \langle m|n\rangle_\mp = 0 \quad (29)$$

2.4 Spectral Triple : Fuzzy Sphere

For the fuzzy sphere the spectral triple was already constructed in [4]. We will be working with the same one here. The spectral triple consists of the algebra $\mathcal{A} \equiv \mathcal{H}_q \ni |m\rangle\langle n|$, the Hilbert space $\mathcal{H} \equiv \mathcal{H}_c \otimes \mathbb{C}^2 \ni \begin{pmatrix} |\psi_1\rangle \\ |\psi_2\rangle \end{pmatrix}$, and the Dirac operator

$$\mathcal{D} \equiv \frac{1}{r_n} \hat{J} \otimes \vec{\sigma} = \frac{1}{r_n} \begin{pmatrix} \hat{J}_3 & \hat{J}_- \\ \hat{J}_+ & -\hat{J}_3 \end{pmatrix}, \quad (30)$$

where \hat{J}_i is related to \hat{x}_i by $\hat{J}_i = \frac{1}{\lambda} \hat{x}_i$ and $\hat{J}_\pm = \hat{J}_1 \pm \hat{J}_2$ are the usual ladder operators. As mentioned earlier we will make use of the Dirac eigen-spinors $|n, n_3\rangle_\pm \in \mathcal{H}_c \otimes \mathbb{C}^2$, which for the fuzzy sphere are given by [12]

$$\begin{aligned} |n, n_3\rangle_+ &:= \sqrt{\frac{n+n_3+1}{2n+1}} |n, n_3\rangle \otimes \begin{pmatrix} 1 \\ 0 \end{pmatrix} + \sqrt{\frac{n-n_3}{2n+1}} |n, n_3+1\rangle \otimes \begin{pmatrix} 0 \\ 1 \end{pmatrix}, \\ |n, n'_3\rangle_- &:= -\sqrt{\frac{n-n_3}{2n+1}} |n, n_3\rangle \otimes \begin{pmatrix} 1 \\ 0 \end{pmatrix} + \sqrt{\frac{n+n_3+1}{2n+1}} |n, n_3+1\rangle \otimes \begin{pmatrix} 0 \\ 1 \end{pmatrix}, \end{aligned} \quad (31)$$

with $-n-1 \leq n_3 \leq n$ and $-n \leq n'_3 \leq n-1$. The respective eigenvalues are given by

$$\lambda_{n_3}^+ = \frac{n}{r_n} \quad ; \quad \lambda_{n'_3}^- = -\frac{(n+1)}{r_n} \quad (32)$$

for any n_3 or n'_3 . Thus, the eigenvalues for a particular n representation is independent of n_3 or n'_3 and is responsible for a $(2n+2)$ -fold degeneracy in the positive eigenvalue sector and a $2n$ -fold degeneracy in the negative eigenvalue sector. This can be understood from the tensor product structure of Dirac operator (30) and the Clebsch-Gordon decomposition of a tensor product of a pair of $SU(2)$ representations. For example, if \hat{J} in (30) corresponds to the $n = 1/2$ representation i.e. $\hat{J} = \vec{\sigma}/2$, then it will split into the direct sum of $n = 1$ (triplet) and $n = 0$ (singlet) representations of three and one dimension, respectively.

2.5 Spectral distance *a la* Connes

States ω are positive linear functionals of norm 1 over \mathcal{A} . Pure states play a rather fundamental role and are defined as those functionals that cannot be written as a convex linear combination of two other functionals. The Connes' spectral distance between two states is then defined by

$$\begin{aligned} d(\omega, \omega') &= \sup_{a \in B} |\omega(a) - \omega'(a)|, \\ B &= \{a \in \mathcal{A} : \|[\mathcal{D}, \pi(a)]\|_{op} \leq 1\}, \\ \|\mathcal{A}\|_{op} &= \sup_{\phi \in \mathcal{H}} \frac{\|\mathcal{A}\phi\|}{\|\phi\|}. \end{aligned} \quad (33)$$

An algorithm, adaptable to this Hilbert-Schmidt operatorial formulation and subject to the following conditions :

- The states ω, ω' are normal states (see [21] for the definition),
- The states ω and ω' are separately bounded on B , i.e. $\omega(a) < \infty$ and $\omega'(a) < \infty, \forall a \in B$,
- Let $V_0 = \{a \in \mathcal{A} : \|[\mathcal{D}, \pi(a)]\|_{op} = 0\}$, then the states ω, ω' are such that $\omega(a) - \omega'(a) = 0, \forall a \in V_0$,

was devised to compute Connes' spectral distance [1]. The present analysis will also assume the above conditions. The first two conditions are actually quite mild and just imply that a generic state ω can be represented by a density matrix ρ . Furthermore, if the state ω is pure, then the corresponding density matrix ρ too will be pure. More specifically, to illustrate through an example, let us consider the case of the Moyal plane \mathbb{R}_*^2 - parametrized by the complex number z . It has a one-to-one correspondence with the coherent state $|z\rangle \in \mathcal{H}_c$ (8) or more precisely the density matrix $\rho_z \equiv |z\rangle\langle z| \in \mathcal{H}_q$. Like-wise, the "harmonic oscillator" state $|n\rangle \in \mathcal{H}_c$ (4) is associated with the density matrix $\rho_n \equiv |n\rangle\langle n| \in \mathcal{H}_q$ ¹. Note that both ρ_z and ρ_n can be regarded as pure states in the C^* -algebraic framework and $\mathcal{H}_q = \mathcal{A}$ can indeed be identified with an involutive algebra, which is a dense sub-algebra of a C^* -algebra, where the hermitian conjugation (\dagger) plays the role of involution operator. Since both ρ and a are elements of $\mathcal{A} = \mathcal{H}_q$, the Connes' distance (33) between a pair of states, now represented by density matrices ρ and ρ' , can be recast in terms of the inner product (6) as

$$d(\rho, \rho') = \sup_{a \in B} |(\Delta\rho, a)| \quad ; \quad \Delta\rho = \rho - \rho'. \quad (34)$$

¹Note that here ρ_z or ρ_n are density matrices from the perspective of \mathcal{H}_c and belong to \mathcal{H}_q . They should not be confused with real quantum density matrices, which should be constructed by taking outer products of states $|\psi\rangle \in \mathcal{H}_q$ as $|\psi\rangle\langle\psi|$. The fact that $\rho_z, \rho_n \in \mathcal{H}_q$ allows us to treat them as vectors, facilitating the analysis of the present paper. This is precisely the advantage of this Hilbert-Schmidt operatorial formulation.

On the other hand the third condition implies a certain irreducibility condition, as explained in [1], [4]. In this context, it is worthwhile to recall another important role of the third condition in the present analysis. If this condition were to be violated then we can find an $a_0 \in V_0$ such that $|\omega'(a_0) - \omega(a_0)| \neq 0$. However, since the ball condition (33) places no constraint on $\|a_0\|_{tr}$, it is clear that no upper bound exists for this distance function and the resulting distance diverges. When this condition holds, the spectral distance is always finite. This point was illustrated through the example of the CP^1 model in [4]. This example, which was first considered in [22], is described by the following spectral triple :

$$\mathcal{A} = M_2(\mathbb{C}), \quad \mathcal{H} = \mathbb{C}^2 \quad \text{and} \quad \mathcal{D} = \begin{pmatrix} D_1 & 0 \\ 0 & D_2 \end{pmatrix}. \quad (35)$$

Note that the Dirac operator has been written here in diagonal form with D_1, D_2 being its eigenvalues. It was shown there that the space of pure states corresponds to $\mathbb{S}^2 \cong CP^1$. Now with $D_1 = D_2$, the Dirac operator will become proportional to the identity operator, so that $\|[\mathcal{D}, \pi(a)]\|_{op} = 0 \forall a \in M_2(\mathbb{C})$ holds trivially and no constraint is imposed by the ball condition on any $a \in M_2(\mathbb{C})$, giving rise to infinite distance between any pair of pure states. Even setting $D_1 \neq D_2$ subsequently, one finds that only parts of the algebra and more specifically the off-diagonal elements a_{12} of $a = \begin{pmatrix} a_{11} & a_{12} \\ a_{12}^* & a_{22} \end{pmatrix}$ gets constrained as $|a_{12}| \leq \frac{1}{|D_1 - D_2|}$, whereas no constraint is imposed on the real diagonal elements a_{11} and a_{22} . Consequently, the distance between any pair of states, belonging to different latitudes diverges and distance between those belonging to the same latitude can only be finite and calculated. Furthermore, note that one may also construct states where the second condition is violated i.e. $\omega(a)$ and $\omega'(a)$ are not separately bounded $\forall a \in B$. In this case the spectral distance will also diverge. Indeed, such states were constructed explicitly in [7]. It is a simple matter to verify that the pure state defined by the unit vector ψ' in eq(3.18) of [7] is not bounded on B , but that elements of the algebra with components of the form given in eq(3.16) of [7] lead to divergent results. We are not interested in this kind of pathological states and our entire analysis will be restricted to the cases where the above mentioned conditions hold.

In the next section we take up the issue of this same computation, but for finite distances, by devising an appropriate and a more general algorithm that also corrects the error in [1]. As mentioned earlier, knowledge of the infinitesimal distance is not enough to compute the finite distance between a pair of finitely separated points by integrating along the geodesic connecting these points, if the concerned non-commutative space does not allow one to define a geodesic in the conventional sense. In fact, as we shall see later, although the Moyal plane \mathbb{R}_*^2 allows one to identify the straight line as the geodesic just like the commutative \mathbb{R}^2 , the great circle in the case of fuzzy sphere \mathbb{S}_*^2 can not be identified in this manner.

3 Towards an algorithm to compute finite distances

As mentioned earlier, we consider the particular case where the states in (33) are normal and bounded so that they are representable by density matrices. With this the Connes distance function (34) becomes

$$d(\omega, \omega') = \sup_{a \in B'} |\text{tr}(\Delta \rho a)| = \sup_{a \in B'} |(\Delta \rho, a)|, \quad (36)$$

where, ρ_ω is the density matrix associated with the state ω so that

$$\omega(a) = \text{tr}(\rho_\omega a), \quad \Delta \rho = \rho_\omega - \rho_{\omega'} \quad (37)$$

and

$$(\Delta \rho, a) = \text{tr}((\Delta \rho)^\dagger a) = \text{tr}(\Delta \rho a). \quad (38)$$

We also introduce the following subsets :

$$V_o^\perp = \{a \in \mathcal{A} : \|[\mathcal{D}, \pi(a)]\|_{op} \neq 0\}, \quad (39)$$

$$B' = \{a \in V_o^\perp : \|[\mathcal{D}, \pi(a)]\|_{op} \leq 1\}, \quad (40)$$

$$W = \{a \in \mathcal{A} : (\Delta \rho, a) = 0\}, \quad (41)$$

following the line of reasoning as in [1].

First we find the lower bound. For this, let us make an assumption that the optimal element $a = a_s \in \mathcal{A} = \mathcal{H}_q$ is aligned in a direction which is either parallel or anti-parallel to $\Delta \rho$. Equivalently a_s can be taken to be proportional to $\Delta \rho$. We thus consider the one-parameter family of algebra elements

$$\Lambda = \left\{ a \in \mathcal{A} : a = \lambda \Delta \rho, 0 \leq \lambda \leq \frac{1}{\|[\mathcal{D}, \pi(a)]\|_{op}} \right\} \subset B'.$$

Taking the extremal element $a = \frac{\Delta \rho}{\|[\mathcal{D}, \pi(\Delta \rho)]\|_{op}}$ yields the lower bound as

$$d(\rho, \rho') \geq \frac{\text{tr}((\Delta \rho)^2)}{\|[\mathcal{D}, \pi(\Delta \rho)]\|_{op}}. \quad (42)$$

The same lower bound can be obtained alternatively in a more rigorous manner by noting that the trace-norm of any element within the ball B' (40) is bounded above. To see this, consider an element $a \in B'$ s.t. $\|[\mathcal{D}, \pi(a)]\|_{\text{op}} \leq 1$. Now writing $a = \|a\|_{\text{tr}} \hat{a}$ in terms of the “unit vector” \hat{a} satisfying $\|\hat{a}\|_{\text{tr}} = 1$, allows us to extract $\|\hat{a}\|_{\text{tr}}$ out of this inequality to write $\|a\|_{\text{tr}} \|[\mathcal{D}, \pi(\hat{a})]\|_{\text{op}} \leq 1$ yielding

$$\|a\|_{\text{tr}} \leq \frac{1}{\|[\mathcal{D}, \pi(\hat{a})]\|_{\text{op}}}. \quad (43)$$

Therefore $\|a\|_{\text{tr}}, a \in B'$ is bounded above by

$$\|a\|_{\text{tr}} \leq \frac{1}{s}, \quad s = \inf_{a \in B'} \|[\mathcal{D}, \pi(\hat{a})]\|_{\text{op}}. \quad (44)$$

We can now decompose \hat{a} in a “longitudinal” ($\widehat{\Delta\rho}$) and “transverse” ($\widehat{\Delta\rho}_\perp$) component as $\hat{a} = \cos\theta \widehat{\Delta\rho} + \sin\theta \widehat{\Delta\rho}_\perp$, where $\|\widehat{\Delta\rho}\|_{\text{tr}} = \|\widehat{\Delta\rho}_\perp\|_{\text{tr}} = 1$ and $\widehat{\Delta\rho}_\perp \in W$, is taken to be orthogonal to $\widehat{\Delta\rho}$ i.e. $(\widehat{\Delta\rho}_\perp, \widehat{\Delta\rho}) = \text{tr}(\widehat{\Delta\rho}_\perp \widehat{\Delta\rho}) = 0$ and corresponds to a unit vector in the plane formed by \hat{a} and $\widehat{\Delta\rho}$. It is clear from (36), that we can choose θ to be an acute angle i.e $0 \leq \theta < \frac{\pi}{2}$, ensuring that both $\sin\theta, \cos\theta$ are positive. Note that here $\cos\theta \neq 0$ since we want $(d\rho, \hat{a}) \neq 0$ otherwise $d(\omega, \omega')$ in (36) would collapse to zero. We can then re-write $\|[\mathcal{D}, \pi(\hat{a})]\|_{\text{op}}$, as in [1] and invoke the triangular inequality to get

$$\|[\mathcal{D}, \pi(\hat{a})]\|_{\text{op}} = \left\| \left[\mathcal{D}, \cos\theta \pi(\widehat{\Delta\rho}) + \sin\theta \pi(\widehat{\Delta\rho}_\perp) \right] \right\|_{\text{op}} \leq |\cos\theta| \left\| \left[\mathcal{D}, \pi(\widehat{\Delta\rho}) \right] \right\|_{\text{op}} + |\sin\theta| \left\| \left[\mathcal{D}, \pi(\widehat{\Delta\rho}_\perp) \right] \right\|_{\text{op}}. \quad (45)$$

This, however, just means that the infimum of the L.H.S is bounded from above as

$$\inf_{\theta \in [0, \pi/2]} \|[\mathcal{D}, \pi(\hat{a})]\|_{\text{op}} \leq \inf_{\theta \in [0, \pi/2]} \left\{ |\cos\theta| \left\| \left[\mathcal{D}, \pi(\widehat{\Delta\rho}) \right] \right\|_{\text{op}} + |\sin\theta| \left\| \left[\mathcal{D}, \pi(\widehat{\Delta\rho}_\perp) \right] \right\|_{\text{op}} \right\} = \min\left\{ \left\| \left[\mathcal{D}, \pi(\widehat{\Delta\rho}) \right] \right\|_{\text{op}}, \left\| \left[\mathcal{D}, \pi(\widehat{\Delta\rho}_\perp) \right] \right\|_{\text{op}} \right\}. \quad (46)$$

Here, of course, the mod over $\sin\theta$ and $\cos\theta$ are quite redundant, as θ is an acute angle as we have mentioned above. Since $\cos\theta \neq 0$, we are forced to identify

$$\inf_{\theta \in [0, \pi/2]} \left\{ |\cos\theta| \left\| \left[\mathcal{D}, \pi(\widehat{\Delta\rho}) \right] \right\|_{\text{op}} + |\sin\theta| \left\| \left[\mathcal{D}, \pi(\widehat{\Delta\rho}_\perp) \right] \right\|_{\text{op}} \right\} = \left\| \left[\mathcal{D}, \pi(\widehat{\Delta\rho}) \right] \right\|_{\text{op}}.$$

Thus, using (44),(45), (46) we observe that s is just bounded from above by $\|[\mathcal{D}, \pi(\widehat{\Delta\rho})]\|_{\text{op}}$

$$s \leq \|[\mathcal{D}, \pi(\widehat{\Delta\rho})]\|_{\text{op}}, \quad (47)$$

but cannot be identified, as was done in [1], with it *in general*. Thus the RHS of (42) was erroneously identified as an upper bound in [1].

Recall in this context that by definition of the infimum, it should rather correspond to the highest lower bound say C , satisfying

$$C \leq \left\| \cos\theta \left[\mathcal{D}, \pi(\widehat{\Delta\rho}) \right] + \sin\theta \left[\mathcal{D}, \pi(\widehat{\Delta\rho}_\perp) \right] \right\|_{\text{op}} \quad \forall \quad \Delta\rho_\perp \in W, \quad \theta \in [0, \pi/2). \quad (48)$$

Since the determination of a general formula to obtain C is difficult, we have to be content with just writing

$$s = \inf_{a \in B'} \|[\mathcal{D}, \pi(\hat{a})]\|_{\text{op}} = \inf_{\Delta\rho_\perp \in W, \theta \in [0, \pi/2)} \left\| \cos\theta \left[\mathcal{D}, \pi(\widehat{\Delta\rho}) \right] + \sin\theta \left[\mathcal{D}, \pi(\widehat{\Delta\rho}_\perp) \right] \right\|_{\text{op}} \quad (49)$$

and find s case by case.

Returning to our derivation, we begin by rewriting the infinitesimal Connes distance function (36),(37) as

$$\begin{aligned} d(\rho, \rho') &= \sup_{a \in B'} |(\Delta\rho, a)| = \sup_{a \in B'} \|a\|_{\text{tr}} |(\Delta\rho, \hat{a})|; \quad \Delta\rho = \rho - \rho' \\ &= \sup_{a \in B'} \|a\|_{\text{tr}} \left| (\Delta\rho, \cos\theta \widehat{\Delta\rho} + \sin\theta \widehat{\Delta\rho}_\perp) \right| = \tilde{N} \|\Delta\rho\|_{\text{tr}}, \end{aligned} \quad (50)$$

where \tilde{N} is given by

$$\tilde{N} = \sup_{a \in B'} (\|a\|_{\text{tr}} |\cos\theta|). \quad (51)$$

In order to determine \tilde{N} , we note that the factors of $\cos\theta$ and $\|a\|_{\text{tr}}$ in \tilde{N} have opposing tendencies in the sense that θ will tend towards zero and θ_c respectively in the factors of $|\cos\theta|$ and $\|a\|_{\text{tr}}$, in their attempt to attain their respective supremum. Consequently, their product as appears here in \tilde{N} (51), will attain the supremum at some intermediate value of θ , say $\theta = \theta_s$ in the interval $0 < \theta_s < \theta_c$, in general. It is therefore desirable to combine these factors and rewrite $d(\rho, \rho')$. For that we use (44, 49) to recast \tilde{N} as

$$\tilde{N} = \frac{1}{\inf_{\substack{\Delta\rho_\perp \in W \\ \theta \in [0, \pi/2)}} \left\| \left[\mathcal{D}, \pi(\widehat{\Delta\rho}) \right] + \tan\theta \left[\mathcal{D}, \pi(\widehat{\Delta\rho}_\perp) \right] \right\|_{\text{op}}} \quad (52)$$

with $\tan \theta$ varying within the range $0 \leq \tan \theta < \infty$.

Here too we can invoke the triangle-inequality to write

$$\|[\mathcal{D}, \pi(\widehat{\Delta\rho})] + \tan \theta [\mathcal{D}, \pi(\widehat{\Delta\rho}_\perp)]\|_{\text{op}} \leq \|[\mathcal{D}, \pi(\widehat{\Delta\rho})]\|_{\text{op}} + |\tan \theta| \|[\mathcal{D}, \pi(\widehat{\Delta\rho}_\perp)]\|_{\text{op}} \quad (53)$$

with the R.H.S. being a monotonically increasing function of θ . This implies that its value at $\theta = 0$ yields the upper bound of the L.H.S. Correspondingly, this yields back the lower bound (42). Finally, we can eliminate the unit vectors $\widehat{\Delta\rho}$ and $\widehat{\Delta\rho}_\perp$ in the ‘‘longitudinal’’ and ‘‘transverse’’ directions respectively to re-write the formula (50-52) in terms of the original vectors $\Delta\rho$ and $\Delta\rho_\perp$ themselves, by multiplying both numerator and denominator by $\|\Delta\rho\|_{\text{tr}}$ to get

$$d(\rho, \rho + \Delta\rho) = N \|\Delta\rho\|_{\text{tr}}^2 = \tilde{N} \|\Delta\rho\|_{\text{tr}}, \quad (54)$$

where

$$N = \frac{1}{\inf_{\Delta\rho_\perp \in W, \kappa \in [0, \infty)} \|[\mathcal{D}, \pi(\Delta\rho)] + \kappa[\mathcal{D}, \Delta\rho_\perp]\|_{\text{op}}} ; \quad \kappa = \frac{\|\Delta\rho\|_{\text{tr}}}{\|\Delta\rho_\perp\|_{\text{tr}}} \tan \theta. \quad (55)$$

From (36) it is clear that the Connes’ distance function can only depend on $\Delta\rho$, i.e.

$$d(\rho, \rho + \Delta\rho) = d(\Delta\rho). \quad (56)$$

It is also elementary to see that for any unitary transformation U

$$d(U\Delta\rho U^\dagger) = d(\Delta\rho). \quad (57)$$

This also implies, from (54), that

$$\tilde{N}(U\Delta\rho U^\dagger) = \tilde{N}(\Delta\rho), \quad N(U\Delta\rho U^\dagger) = N(\Delta\rho). \quad (58)$$

In general we note from (52) and (55) that N and \tilde{N} depend on the ‘direction’ of $\Delta\rho$, in the sense that even if $\|\Delta\rho'\|_{\text{tr}} = \|\Delta\rho\|_{\text{tr}}$, $N(\Delta\rho') \neq N(\Delta\rho)$. However, if $\|\Delta\rho'\|_{\text{tr}} = \|\Delta\rho\|_{\text{tr}}$ implies $\Delta\rho' = U\Delta\rho U^\dagger$, this dependence disappears using (58), \tilde{N} is a constant as $\widehat{\Delta\rho}'$ and $\widehat{\Delta\rho}$ both have norm one and $N = \frac{\tilde{N}}{\|\Delta\rho\|_{\text{tr}}}$. This is the case for the coherent state basis in the Moyal plane, where equality of the trace norms implies that $\Delta\rho'$ and $\Delta\rho$ differ by a rotation of the form $R = e^{i\phi b^\dagger b}$. This explains why the Connes’ distance on the Moyal plane is proportional to the trace norm, which is simply the Euclidean distance, infinitesimally and for finite distances. We corroborate this result in the next section through a more explicit calculation.

More generally, it is not difficult to verify that $\|\Delta\rho'\|_{\text{tr}} = \|\Delta\rho\|_{\text{tr}}$ implies $\Delta\rho' = U\Delta\rho U^\dagger$ if $\Delta\rho$ and $\Delta\rho'$ are the difference of two orthogonal pure states, in which case \tilde{N} is again a constant. This, and more general scenarios under which this holds will be explored elsewhere.

However, this clearly cannot hold in general, but when this is the case, it readily follows that \tilde{N} , as determined from (52) indeed corresponds to a numerical constant and upto this constant (51) the metric g_{ij} that can be read off from the infinitesimal distance (50), is indeed given by the Provost-Vallee form i.e. $g_{ij} \propto (\partial_i \rho, \partial_j \rho)$ [1, 16] in the coherent state basis in particular. In the case of the Moyal plane, this readily yields a flat metric, as in [1], so that the straight lines are expected to play the role of geodesics. Indeed this fact was used implicitly in the parametrization (61) below. On the other hand, for the case of the fuzzy sphere, although the metric is that of commutative sphere - upto an overall numerical factor, it turns out that the finite distance is quite different from the geodesic (great circle). Indeed, for the $n = 1/2$ representation of $SU(2)$ i.e. for the case of maximal non-commutativity, the distance turns out to be half of the chordal distance [12] and there does not exist any geodesic in the conventional sense, preventing one to integrate the infinitesimal distance to compute finite distance and the commutative result is obtained only in the $n \rightarrow \infty$ limit. As we shall see in the sequel essentially similar results are obtained by applying our formula (54). We begin with the computation of the finite distance between coherent states on the Moyal plane in the next section.

4 Distance between finitely separated coherent states in \mathbb{R}_*^2

The purpose of this section is to determine the spectral distance, *a la* Connes, between an arbitrary pair of finitely separated coherent states $|z\rangle, |z'\rangle \in \mathcal{H}_c$, or more precisely between $\rho_z = |z\rangle\langle z|$ and $\rho_{z'} = |z'\rangle\langle z'| \in \mathcal{A} = \mathcal{H}_q$. Although a formal algorithm (54) and (55) was devised for this purpose in the preceding section, this is not very user-friendly, as the identification of the right $\Delta\rho_\perp$, for which the infimum is reached in (55) is an extremely difficult job. On the other hand, the lower bound (42) can be easily computed as was done in [1, 4] (at most up to a numerical constant). The strategy we therefore adopt is to emulate [2] to obtain the corresponding upper bound and then look for an optimal element a_s for which the saturation condition holds. If we can identify at least one a_s (note that this may not be unique!) then we can identify the upper bound to be the true distance. It may also happen in some situations that both upper and lower bounds coincide. In this case, their common value can be identified as the distance. Otherwise, one has to play with different choices of $\Delta\rho_\perp$ in (55) to find the best possible estimate, as the upper bound cannot be identified as the true distance. We shall encounter a variety of such situations in the rest of the paper, which will help

us to study and contrast various non-commutative spaces through the examples of \mathbb{R}_*^2 and \mathbb{S}_*^2 . The present section deals with \mathbb{R}_*^2 .

We begin by considering the action of the state ω_z , (associated to the fuzzy point z in the Moyal plane, in the spirit of Gelfand and Naimark), on a generic algebra element $a \in \mathcal{H}_q$ as,

$$\begin{aligned}\omega_z(a) &= \text{tr}(\rho_z a) = \text{tr}(U(z, \bar{z})|0\rangle\langle 0|U^\dagger(z, \bar{z})a) \\ &= \langle 0|(U^\dagger(z, \bar{z})aU(z, \bar{z}))|0\rangle.\end{aligned}\tag{59}$$

Note that we have made use of (8) here. This means that the algebra element $a \in \mathcal{A} = \mathcal{H}_q$ gets translated by the adjoint action of $U(z, \bar{z})$ thereby furnishing a proper representation of the translation group. Without loss of generality we therefore only have to compute the distance between the pair of states ω_z and ω_0 (taken to correspond to the ‘‘origin’’ $z = 0$) as can easily be seen by invoking the transformational property of the Dirac operator \mathcal{D} under translation (236), (as explained in Appendix A) and can be written, by using (33), as

$$d(\omega_z, \omega_0) = \sup_{a \in \mathcal{B}} |\langle 0|(U^\dagger(z, \langle z|)aU(z, \langle z|))|0\rangle - \langle 0|a|0\rangle|.\tag{60}$$

Intuitively, $d(\omega_z, \omega_0)$ is the maximum change in the expectation values of the $a \in \mathcal{B}$ and the translated algebra element $U^\dagger(z, \langle z|)aU(z, \langle z|)$ in the same state $|0\rangle \in \mathcal{H}_c$. This is somewhat reminiscent of the transition from the Schrödinger to Heisenberg picture, where the operators are subjected to the unitary evolution in time through an adjoint action of the unitary operator, while the states are held frozen in time.

To proceed further, let us introduce a one-parameter family of density matrices $\rho_{zt} = |zt\rangle\langle zt|$ with $t \in [0, 1]$ taken to be, for convenience, a real affine parameter along the straight line connecting the origin $z = 0$ and the point z in the complex plane. We can then introduce

$$W(t) = \omega_{zt}(a) = \text{tr}(\rho_{zt}a).\tag{61}$$

Consequently, we have the following inequality,

$$|\omega_z(a) - \omega_0(a)| = \left| \int_0^1 \frac{dW(t)}{dt} dt \right| \leq \int_0^1 \left| \frac{dW(t)}{dt} \right| dt.\tag{62}$$

Since

$$\frac{dW(t)}{dt} = \frac{d(\omega_{zt}(a))}{dt} = \frac{d\langle 0|(U^\dagger(zt, \langle z|t) a U(zt, \langle z|t))|0\rangle}{dt},$$

we can make use of the Hadamard identity

$$\begin{aligned}(U^\dagger(z, \bar{z})aU(z, \bar{z})) &= \exp(G)a\exp(-G) \\ &= a + [G, a] + \frac{1}{2!}[G, [G, a]] + \frac{1}{3!}[G, [G, [G, a]]] + \dots,\end{aligned}\tag{63}$$

where $G = \bar{z}b - zb^\dagger$, to get

$$\begin{aligned}\frac{dW(t)}{dt} &= \langle 0|[G, a]|0\rangle + t\langle 0|[G, [G, a]]|0\rangle + \frac{t^2}{2!}\langle 0|[G, [G, [G, a]]]|0\rangle + \dots \\ &= \langle 0|(\exp(tG)[G, a]\exp(-tG))|0\rangle.\end{aligned}$$

On further simplification, this can be recast as

$$\frac{dW(t)}{dt} = |\bar{z}\omega_{zt}([b, a]) + z\omega_{zt}([b, a]^\dagger)|\tag{64}$$

since only a hermitian element ($a = a^\dagger \in \mathcal{A}$) can give the supremum in the Connes’ distance function [22]. This yields an upper bound for $|\frac{dW(t)}{dt}|$ by making use of the Cauchy-Schwarz inequality:

$$\left| \frac{dW(t)}{dt} \right| = |\bar{z}\omega_{zt}([b, a]) + z\omega_{zt}([b, a]^\dagger)|\tag{65}$$

$$\leq \sqrt{2}|z|\sqrt{|\omega_{zt}([b, a])|^2 + |\omega_{zt}([b, a]^\dagger)|^2}\tag{66}$$

$$\leq \sqrt{2}|z|\sqrt{\|[b, a]\|_{op}^2 + \|[b, a]^\dagger\|_{op}^2}\tag{67}$$

Note that in the last step, we have made use of the fact that states ω ’s are linear functionals of unit norm.

Now with the Dirac operator \mathcal{D} (26), one can prove [see Appendix A.1] the following identity

$$\|[\mathcal{D}, \pi(a)]\|_{op} = \sqrt{\frac{2}{\theta}} \| [b, a] \|_{op} = \sqrt{\frac{2}{\theta}} \| [b^\dagger, a] \|_{op}. \quad (68)$$

Using this, the ‘‘ball’’ condition (33) reduces for $a \in B$ to

$$\| [b, a] \|_{op} = \| [b^\dagger, a] \|_{op} \leq \sqrt{\frac{\theta}{2}}. \quad (69)$$

From (67) and (69), one can therefore write

$$\left| \frac{dW(t)}{dt} \right| \leq \sqrt{2\theta} |z|. \quad (70)$$

Hence from eq (33), (62 and (70) we have the following upper bound for the Connes’ distance:

$$d(\omega_z, \omega_0) \leq \sqrt{2\theta} |z|. \quad (71)$$

Clearly, the RHS can be identified as the Connes’ distance, provided there exists an optimal element $a_s \in B$ for which the inequality of (71) is saturated. We therefore look for an optimal element $a = a_s$, satisfying $U^\dagger a_s U = (a_s + \sqrt{2\theta}|z|)$ s.t.

$$d(\omega_z, \omega_0) = \sqrt{2\theta} |z|. \quad (72)$$

A simple inspection of (63) shows that a_s should satisfy

$$[G, a_s] = \sqrt{2\theta}|z| \quad \text{and} \quad [G, [G, a_s]] = 0, \quad (73)$$

where $G = \bar{z}b - zb^\dagger$, ensuring that all higher order nested commutators vanish. Observe that since b, b^\dagger act irreducibly on \mathcal{H}_c , we must have, using Schur’s lemma, $[G, a_s]$ to be proportional to the identity operator, as happens here. This yields,

$$a_s = \sqrt{\frac{\theta}{2}} (be^{-i\alpha} + b^\dagger e^{i\alpha}), \quad (74)$$

where $z = |z|e^{i\alpha}$.

One can check at this stage that although $a_s \in B$

$$\|[\mathcal{D}, \pi(a_s)]\|_{op} = 1, \quad (75)$$

it fails to be a trace-class operator :

$$\|a_s\|_{tr} = \sqrt{\frac{\theta}{2}} \sum_{n=0}^{\infty} (2n+1) = \infty. \quad (76)$$

Consequently $a_s \notin \mathcal{H}_q = \mathcal{A}$, but can be thought of as belonging to the multiplier algebra². A resolution of this problem was provided in [2]. We briefly describe their approach here, as we propose an alternative approach in the next sub-section.

Here one weakens the strong requirement that $a_s \in \mathcal{H}_q = \mathcal{A}$ and rather looks for a sequence $\{a_n\}$, $a_n \in B$ and also $a_n \in \mathcal{A} = \mathcal{H}_q$, by inserting a suitable operator-valued ‘‘Gaussian’’ factor to ensure convergence of the trace-norm and thereby rendering it a trace-class operator:

$$a_n = \sqrt{\frac{\theta}{2}} \left(be^{-i\alpha} (e^{-\lambda_n b^\dagger b}) + (e^{-\lambda_n b^\dagger b}) b^\dagger e^{i\alpha} \right). \quad (77)$$

Then the following proposition was proved in [2] (proposition 3.5):

Proposition:

Let $z = |z|e^{i\alpha}$ be a fixed translation and $\lambda > 0$. Define $a = \sqrt{\frac{\theta}{2}} (b' + b'^\dagger)$, where $b' = be^{-i\alpha} (e^{-\lambda b^\dagger b})$. Then there exists a $\gamma > 0$ s.t. $a \in B$ (Lipschitz ball) for any $\lambda \leq \gamma$.

Using this proposition, any generic element of the sequence (77) can be written in terms of above b' as

$$a = \sqrt{\frac{\theta}{2}} (b' + b'^\dagger) \in B \quad \text{with} \quad \lambda \leq \gamma.$$

Now, it can be easily shown that

$$\omega_0(a) = 0 \quad \text{and} \quad \omega_z(a) = \sqrt{2\theta} |z| \exp(-|z|^2(1 - e^{-\lambda})).$$

Therefore,

$$d(\omega_z, \omega_0) = \lim_{n \rightarrow \infty} |\omega_z(a) - \omega_0(a)| = \lim_{\lambda \rightarrow 0} |\omega_z(a) - \omega_0(a)| = \lim_{\lambda \rightarrow 0} \sqrt{2\theta} |z| \exp(-|z|^2(1 - e^{-\lambda})) = \sqrt{2\theta} |z|. \quad (78)$$

²Multiplier algebra $M = M_L \cap M_R$ where $M_L = \{T \mid \psi T \in \mathcal{H}_q \forall \psi \in \mathcal{H}_q\}$ and $M_R = \{T \mid T\psi \in \mathcal{H}_q \forall \psi \in \mathcal{H}_q\}$

4.1 Infinitesimal distance and optimal element

It is clear, on the other hand, from the translational symmetry of the Dirac operator \mathcal{D} (26) (see appendix A) that it is quite adequate to look for the optimal element a_s at the level of the infinitesimal distance itself. The anticipated advantage is that a_s (74) when projected to a finite dimensional sub-space will be automatically trace-class. Besides, it will help us to put the computation presented in [1] in the context of the present analysis and to zoom in on the source of the mismatch between the result of [1] and [7], by a factor of $\sqrt{3}$. We therefore turn our attention towards the computation of the Connes distance between infinitesimally separated coherent states $\rho_z = |z\rangle$ and ρ_{z+dz} . Clearly, this can just be read off from (72) to yield, by invoking translational symmetry (see Appendix A.1),

$$d(\rho_0, \rho_{dz}) = d(\rho_z, \rho_{z+dz}) = \sqrt{2\theta}|dz| \quad (79)$$

and the apparent optimal element for the infinitesimal case is easily obtained by projecting a_s (74) into the 2D subspace $\text{Span}\{|0\rangle, |1\rangle\}$ to get

$$a_s^{eff} = P_2 a_s P_2 = \sqrt{\frac{\theta}{2}} \frac{d\rho}{|dz|}; \quad P_2 \equiv (|0\rangle\langle 0| + |1\rangle\langle 1|), \quad (80)$$

where

$$d\rho = \rho_{dz} - \rho_0 = |dz\rangle\langle dz| - |0\rangle\langle 0| = d\bar{z}|0\rangle\langle 1| + dz|1\rangle\langle 0| \quad (81)$$

upto $\mathcal{O}(dz^2, d\bar{z}^2)$. Note that the projection P_2 was employed to construct a_s^{eff} (80), as $d\rho$ (81) lives in the above-mentioned 2D subspace and consequently only the projected component of a_s (74) can contribute to the distance, given in terms of the inner product (34). We therefore observe that in this case we have to deal with only finite dimensional subspaces, the optimal element is trace-class, $a_s^{eff} \in \mathcal{A} = \mathcal{H}_q$ by default and we need not invoke any sequence here. However, in this case it does not belong to the ball B (33) any more: $\|[\mathcal{D}, a_s^{eff}]\|_{op} = \sqrt{3} > 1 \implies a_s \notin B$. In other words, (79) can just be written as

$$d(\rho_0, \rho_{dz}) = (d\rho, a_s^{eff}) = \sqrt{2\theta}|dz|, \quad (82)$$

the difference with (34) being the *absence* of the ball condition: $a_s \in B$; all that we have is $a_s^{eff} \in \mathcal{A} = \mathcal{H}_q$. This situation is therefore quite opposite to the finite case where $a_s \in B$ (75) but $a_s \notin \mathcal{A} = \mathcal{H}_q$ (76). This a_s^{eff} (80) therefore cannot be identified with the *true* optimal element. This a_s^{eff} can, at best, be identified as an *effective optimal* element. One way to try to remedy this situation would be to replace a_s^{eff} by $a_s^{eff}/\sqrt{3}$ as this will now satisfy the ball condition. This results in the distance expression $d(\rho_z, \rho_{z+dz}) = \sqrt{\frac{2\theta}{3}}|dz|$, thus reproducing the result of [1]. One can, however, recognise easily that the occurrence of the $\sqrt{3}$ factor violating the ball condition is just an artefact of this inappropriate projection procedure. To see it more transparently, let us project the infinite dimensional matrix a_s to a more general, but finite (say $N+1$)-dimensional subspace of \mathcal{H}_q by $P_{N+1} = \sum_{n=0}^N |n\rangle\langle n|$, and then compute $[\mathcal{D}, \pi(P_{N+1} a_s P_{N+1})]^\dagger [\mathcal{D}, \pi(P_{N+1} a_s P_{N+1})]$. We find the matrix to be living on a higher $(N+2)$ -dimensional subspace, having a block-diagonal form:

$$[b, P_{N+1} a_s P_{N+1}]^\dagger [b, P_{N+1} a_s P_{N+1}] = \frac{\theta}{2} \left(\begin{array}{c|c} \mathbb{1}_{(N-1) \times (N-1)} & 0_{(N-1) \times 3} \\ \hline 0_{3 \times (N-1)} & A \end{array} \right), \quad (83)$$

but with A being a 3×3 non-diagonal block matrix:

$$A = \begin{pmatrix} 1 & 0 & \sqrt{N(N+1)} \\ 0 & 0 & 0 \\ \sqrt{N(N+1)} & 0 & N(N+1) \end{pmatrix}. \quad (84)$$

The corresponding operator norm thus turns out to be a linearly divergent N -dependent function $\sqrt{N(N+1)+1} > 1$. For $N=1$ this is just $\sqrt{3}$ as mentioned above. Thus, although $d\rho$ (81) and a_s^{eff} (80) are proportional, the inappropriate projector P_2 (80) generates the undesirable $\sqrt{3}$ factor, otherwise the lower bound (42) itself would have yielded the desired result (79).

We now present an alternative to this ‘‘Gaussian’’ sequence approach of (77)-(78) [2] by constructing a sequence of projected $\pi(a_s)$ in $\mathcal{H}_q \otimes M_2(\mathbb{C})$, rather than projected a_s in \mathcal{H}_q as in (80), using a projector which is appropriate for the eigen-spinor basis of the Dirac operator (28). This will allow us to evade the problem associated with the violation of the ball condition projector P_N (83) for \mathcal{H}_q only.

We begin with the diagonal representation of $a \in \mathcal{A} = \mathcal{H}_q$, i.e. $\pi(a) = \begin{pmatrix} a & 0 \\ 0 & a \end{pmatrix} \in \mathcal{H}_q \otimes M_2(\mathbb{C})$. In particular for $a = d\rho$ (81), we have

$$\pi(d\rho) \equiv \begin{pmatrix} d\rho & 0 \\ 0 & d\rho \end{pmatrix} = \begin{pmatrix} 0 & \frac{d\bar{z}}{\sqrt{2}} & \frac{d\bar{z}}{\sqrt{2}} & 0 & 0 \\ \frac{dz}{\sqrt{2}} & 0 & 0 & \frac{d\bar{z}}{2} & -\frac{dz}{2} \\ \frac{dz}{\sqrt{2}} & 0 & 0 & -\frac{d\bar{z}}{2} & \frac{dz}{2} \\ 0 & \frac{dz}{2} & -\frac{dz}{2} & 0 & 0 \\ 0 & -\frac{dz}{2} & \frac{dz}{2} & 0 & 0 \end{pmatrix} \in \mathcal{H}_q \otimes M_2(\mathbb{C}), \quad (85)$$

where the columns and rows are labelled by $|0\rangle, |1\rangle_+, |1\rangle_-, |2\rangle_+, |2\rangle_-$ of (28), respectively. Note that it has vanishing entries in the remaining rows/columns, indexed by $|n\rangle_\pm$, with $n \geq 3$.

Proceeding with the same proposed optimal element (74), we now project it on the representation space spanned by the eigen-spinors. To begin with, we first project it on the same above 5D subspace spanned by $|0\rangle, |1\rangle_\pm, |2\rangle_\pm$.

$$\pi(a_s) \rightarrow \mathbb{P}_2 \pi(a_s) \mathbb{P}_2 \quad \text{with} \quad \mathbb{P}_2 = |0\rangle\langle 0| + |1\rangle_+\langle 1|_+ + |1\rangle_-\langle 1|_- - |2\rangle_+\langle 2|_+ + |2\rangle_-\langle 2|_- - |2\rangle_\pm\langle 2|_\pm. \quad (86)$$

On computation this yields

$$\mathbb{P}_2 \pi(a_s) \mathbb{P}_2 = \sqrt{\frac{\theta}{2}} \begin{pmatrix} 0 & \frac{1}{\sqrt{2}} & \frac{1}{\sqrt{2}} & 0 & 0 \\ \frac{1}{\sqrt{2}} & 0 & 0 & \frac{\sqrt{2}+1}{2} & \frac{\sqrt{2}-1}{2} \\ \frac{1}{\sqrt{2}} & 0 & 0 & \frac{\sqrt{2}-1}{2} & \frac{\sqrt{2}+1}{2} \\ 0 & \frac{\sqrt{2}+1}{2} & \frac{\sqrt{2}-1}{2} & 0 & 0 \\ 0 & \frac{\sqrt{2}-1}{2} & \frac{\sqrt{2}+1}{2} & 0 & 0 \end{pmatrix}. \quad (87)$$

Consequently,

$$[\mathcal{D}, \mathbb{P}_2 \pi(a_s) \mathbb{P}_2] \equiv \begin{pmatrix} 0 & -\frac{1}{\sqrt{2}} & \frac{1}{\sqrt{2}} & 0 & 0 \\ \frac{1}{\sqrt{2}} & 0 & 0 & -\frac{1}{2} & \frac{1}{2} \\ -\frac{1}{\sqrt{2}} & 0 & 0 & -\frac{1}{2} & \frac{1}{2} \\ 0 & \frac{1}{2} & \frac{1}{2} & 0 & 0 \\ 0 & -\frac{1}{2} & -\frac{1}{2} & 0 & 0 \end{pmatrix} \quad (88)$$

and finally, in contrast to (83), we have

$$[\mathcal{D}, \mathbb{P}_2 \pi(a_s) \mathbb{P}_2]^\dagger [\mathcal{D}, \mathbb{P}_2 \pi(a_s) \mathbb{P}_2] \equiv \left(\begin{array}{c|c} \mathbb{1}_{3 \times 3} & \mathbb{0}_{3 \times 2} \\ \hline \mathbb{0}_{2 \times 3} & B_{2 \times 2} \end{array} \right), \quad (89)$$

where

$$B = \begin{pmatrix} 1/2 & -1/2 \\ -1/2 & 1/2 \end{pmatrix} \quad (90)$$

is a 2×2 square matrix having eigenvalues 1 and 0. This is in contrast to the matrix A (84). Further, $O_{m \times n}$ refers to a rectangular null matrix with m rows and n columns. Thus clearly we have in this case,

$$\|[\mathcal{D}, \mathbb{P}_2 \pi(a_s) \mathbb{P}_2]\|_{op} = 1 \quad (91)$$

and,

$$\frac{1}{2} |\langle \langle \pi(d\rho) | \mathbb{P}_2 \pi(a_s) \mathbb{P}_2 \rangle \rangle| = \sqrt{2\theta} |dz|, \quad (92)$$

where $\langle \langle \cdot | \cdot \rangle \rangle$ denotes the inner product between a pair of elements $\mathcal{H}_q \otimes M_2(\mathbb{C})$ given by

$$\langle \langle A_1 | A_2 \rangle \rangle = \text{Tr}_{\mathcal{H}_c \otimes \mathbb{C}^2} (A_1^\dagger A_2) \quad ; \quad A_1, A_2 \in \mathcal{H}_q \otimes M_2(\mathbb{C}) \quad (93)$$

and is the counter part of (6). Again, the subscript $\mathcal{H}_c \otimes \mathbb{C}^2$ indicates that the trace has to be computed over $\mathcal{H}_c \otimes \mathbb{C}^2$. Further note that a factor of $1/2$ has been inserted in (92) in anticipation to relate the inner products (6) and (93), in case both A_1 and A_2 in (91) are representations of $a_1, a_2 \in \mathcal{H}_q$ such that $A_1 = \pi(a_1)$ and $A_2 = \pi(a_2)$. In that case, they can be related as, $(a_1, a_2) = \frac{1}{2} \langle \langle \pi(a_1) | \pi(a_2) \rangle \rangle$. Of course here one can easily see that \nexists any $a \in \mathcal{H}_q$ s.t. $\pi(a) = \mathbb{P}_2 \pi(a_s) \mathbb{P}_2$ and one can not simply relate (93) with any inner products (\cdot, \cdot) of \mathcal{H}_q . Indeed, if it were to exist, we could have identified this 'a', using (91) and (92), to be the optimal element itself, which by definition has to belong to $\mathcal{H}_q = \mathcal{A}$, or at best to the multiplier algebra. In fact, this will be a persistent feature with any finite $(2N + 1)$ -dimensional projection $\mathbb{P}_N \pi(a_s) \mathbb{P}_N$ with

$$\mathbb{P}_N = |0\rangle\langle 0| + \sum_{n=1, \pm}^N |n\rangle_\pm \langle n|_\pm. \quad (94)$$

One can note at this stage, however, that one can keep on increasing the rank of the projection operator \mathbb{P}_N indefinitely without affecting (91) and (92) in the sense that the counter part of these equations still has the same form

$$\|[\mathcal{D}, \mathbb{P}_N \pi(a_s) \mathbb{P}_N]\|_{op} = 1 \quad (95)$$

and

$$\frac{1}{2} |\langle \langle \pi(d\rho) | \mathbb{P}_N \pi(a_s) \mathbb{P}_N \rangle \rangle| = \sqrt{2\theta} |dz| \quad (96)$$

are independent of N if $N \geq 2$.

These equations again follow from the fact that

$$[\mathcal{D}, \mathbb{P}_N \pi(a_s) \mathbb{P}_N]^\dagger [\mathcal{D}, \mathbb{P}_N \pi(a_s) \mathbb{P}_N] = \left(\frac{\mathbf{1}_{(2N-1) \times (2N-1)}}{O_{2 \times (2N-1)}} \mid \frac{O_{(2N-1) \times 2}}{B} \right) \quad (97)$$

with B (90) again appearing as the lower block and $\pi(d\rho)$ (85) has "support" only on the first 5×5 block.

Finally, since in the limit $N \rightarrow \infty$, $\mathbb{P}_N \rightarrow \mathbf{1}$ by (29), we have $\mathbb{P}_N \pi(a_s) \mathbb{P}_N \rightarrow \pi(a_s)$. One can thus interpret

$$\|[\mathcal{D}, \pi(a_s)]\|_{op} \equiv \lim_{N \rightarrow \infty} \|[\mathcal{D}, \mathbb{P}_N \pi(a_s) \mathbb{P}_N]\|_{op} = 1 \quad (98)$$

and

$$(d\rho, a_s) = \frac{1}{2} |\langle \langle \pi(d\rho) \mid \pi(a_s) \rangle \rangle| \equiv \lim_{N \rightarrow \infty} \frac{1}{2} |\langle \langle \pi(d\rho) \mid \mathbb{P}_N \pi(a_s) \mathbb{P}_N \rangle \rangle| = \sqrt{2\theta} |dz|. \quad (99)$$

Thus, instead of inserting a Gaussian factor, as in (77), we have a sequence $\{\mathbb{P}_N \pi(a_s) \mathbb{P}_N\}$ of trace-class operators living in $\mathcal{H}_q \otimes M_2(\mathbb{C})$ (note that $\mathcal{H}_q \otimes M_2(\mathbb{C})$ can be regarded as Hilbert-Schmidt operators acting on $\mathcal{H}_c \otimes \mathbb{C}^2$) and each of them satisfy the ball condition (95). This is accomplished by projecting in the finite dimensional subspaces spanned by Dirac eigen-spinors (29) rather than projecting just to \mathcal{H}_q by \mathbb{P}_N in (83), where the ball condition gets violated and the operator norm diverges linearly. This latter projector could be associated naturally to a different orthonormal and complete basis

$$\left\{ |n, \uparrow\rangle = |n\rangle \otimes \begin{pmatrix} 1 \\ 0 \end{pmatrix} = \begin{pmatrix} |n\rangle \\ 0 \end{pmatrix} ; |n, \downarrow\rangle = |n\rangle \otimes \begin{pmatrix} 0 \\ 1 \end{pmatrix} = \begin{pmatrix} 0 \\ |n\rangle \end{pmatrix} \right\} \quad (100)$$

for $\mathcal{H}_c \otimes \mathbb{C}^2$ as $\mathbb{P}_N \in \mathcal{A} = \mathcal{H}_q$ and $\pi(\mathbb{P}_N)$ has the block-diagonal form $\pi(\mathbb{P}_N) = \begin{pmatrix} \mathbb{P}_N & 0 \\ 0 & \mathbb{P}_N \end{pmatrix} \in \mathcal{H}_q \otimes M_2(\mathbb{C})$. Note that the eigen-spinor basis (29) is easily obtained from (100) by first leaving out $\begin{pmatrix} |0\rangle \\ 0 \end{pmatrix} \equiv |0\rangle$ separately and then pairing $|n, \uparrow\rangle$ and $|n-1, \downarrow\rangle$ as

$$|n\rangle_\pm = \frac{1}{\sqrt{2}} (|n, \uparrow\rangle \pm |n-1, \downarrow\rangle) = \frac{1}{\sqrt{2}} \begin{pmatrix} |n\rangle \\ \pm |n-1\rangle \end{pmatrix}; \quad n = 1, 2, 3, \dots \quad (101)$$

The projector \mathbb{P}_N (94) is then clearly the natural choice for the ball condition due to its natural association with the Dirac operator. Furthermore, note that we have to make use of the entire a_s (74) as the optimal element. We would also like to point out in this context that $\pi(d\rho)$ (85) and $\mathbb{P}_2 \pi(a_s) \mathbb{P}_2$ (87) are not proportional anymore, unlike their counterparts (80). However, here too we can easily split $\mathbb{P}_2 \pi(a_s) \mathbb{P}_2$ or for that matter $\pi(a_s)$ itself in the limit $N \rightarrow \infty$, into the longitudinal and transverse components, but now in $\mathcal{H}_q \otimes M_2(\mathbb{C})$ and not in \mathcal{H}_q . This requires a slight generalization of the analysis presented in section 3. This, however, is not very useful in this context and we do not pursue it here anymore.

It is finally clear from the above analysis that the upper bound (71) is saturated in the infinitesimal case through the sequence $\{\mathbb{P}_N \pi(a_s) \mathbb{P}_N\}$ in the limit $N \rightarrow \infty$, allowing one to identify

$$d(\rho_0, \rho_{dz}) = d(|0\rangle\langle 0|, |dz\rangle\langle dz|) = \sqrt{2\theta} |dz|. \quad (102)$$

Invoking translational symmetry with $U(z, \bar{z})$ as in (8) and the transformational property of the Dirac operator (236), it is clear that

$$d(\rho_0, \rho_{dz}) = d(\rho_z, \rho_{z+dz}) = \sqrt{2\theta} |dz| \quad \forall z \in \{zt, t \in [0, 1]\} \quad (103)$$

and one concludes that for finitely separated states, one can write

$$d(\rho_0, \rho_z) = \sqrt{2\theta} |z|, \quad (104)$$

reproducing the result (78) and identify the straight line joining $z = 0$ to z to be geodesic of the Moyal plane enabling one to integrate the infinitesimal distance (103) along this geodesic to compute finite distance. In fact, one can easily see at this stage that the distance (104) can be written as the sum of distances $d(\rho_0, \rho_{zt})$ and $d(\rho_{zt}, \rho_z)$ as,

$$d(\rho_0, \rho_z) = d(\rho_0, \rho_{zt}) + d(\rho_{zt}, \rho_z), \quad (105)$$

where ρ_{zt} is an arbitrary intermediate pure state from the one-parameter family of pure states, introduced in (61), so that the respective triangle inequality becomes an equality.

As we shall subsequently see this feature will not persist for other generic non-commutative spaces and we will demonstrate this through the example of the fuzzy sphere later. Before that we, however, complete our study of the Moyal plane by computing the distance between the discrete "harmonic oscillator" states in the next section.

5 Connes distance between discrete “harmonic oscillator” states

5.1 Distance between infinitesimally separated discrete “harmonic oscillator” states $|n\rangle$ and $|n+1\rangle$ in the Moyal plane

For the discrete case, we consider a pair of states, which are separated by an “infinitesimal” distance. By this we mean the nearest states, which are eigenstates of $b^\dagger b$. To compute the distance between the states $\rho_{n+1} \equiv |n+1\rangle\langle n+1|$ and $\rho_n \equiv |n\rangle\langle n|$ we take a similar approach i.e. start with

$$d(\omega_{n+1}, \omega_n) = \sup_{a \in B} |\text{tr}(\rho_{n+1} a) - \text{tr}(\rho_n a)| \quad (106)$$

and re-express this as the difference in the expectation value of the transformed algebra element and that of itself in the same state $|n\rangle$ as

$$\begin{aligned} d(\omega_{n+1}, \omega_n) &= \sup_{a \in B} |\langle n | \frac{b}{\sqrt{n+1}} a \frac{b^\dagger}{\sqrt{n+1}} | n \rangle - \langle n | a | n \rangle| \\ &= \sup_{a \in B} \frac{1}{n+1} |\langle n | ([b, a] + ab) b^\dagger - (n+1)a | n \rangle|. \end{aligned}$$

On simplification this yields

$$\begin{aligned} d(\omega_{n+1}, \omega_n) &= \sup_{a \in B} \frac{1}{\sqrt{n+1}} |\langle n | [b, a] | n+1 \rangle| \\ &= \sup_{a \in B} \frac{1}{\sqrt{n+1}} |\langle n+1 | [b^\dagger, a] | n \rangle|. \end{aligned} \quad (107)$$

We can now invoke Bessel’s inequality

$$\|A\|_{op}^2 \geq \sum_i |A_{ij}|^2 \geq |A_{ij}|^2 \quad (108)$$

(written in terms of the matrix elements A_{ij} of an operator \hat{A} in some orthonormal bases), to write (using (68))

$$\begin{aligned} d(\omega_{n+1}, \omega_n) &= \sup_{a \in B} \frac{1}{\sqrt{n+1}} |\langle n | [b, a] | n+1 \rangle| \\ &= \sup_{a \in B} \frac{1}{\sqrt{n+1}} |\langle n+1 | [b^\dagger, a] | n \rangle| \\ &\leq \frac{1}{\sqrt{n+1}} \|[b, a]\|_{op} = \frac{1}{\sqrt{n+1}} \|[b^\dagger, a]\|_{op}. \end{aligned} \quad (109)$$

This finally yields

$$d(\omega_{n+1}, \omega_n) \leq \sqrt{\frac{\theta}{2(n+1)}}. \quad (110)$$

Again the RHS will correspond to the required distance, provided that we can find at least one optimal element a_s s.t. the above inequality is saturated. We try with the lower bound (42):

$$a_s = \frac{d\rho}{\|[\mathcal{D}, \pi(d\rho)]\|_{op}}, \quad (111)$$

where $d\rho = \rho_{n+1} - \rho_n = |n+1\rangle\langle n+1| - |n\rangle\langle n|$. The operator norm $\|[\mathcal{D}, \pi(d\rho)]\|_{op}$ can now be computed using the eigen-spinor basis (28). Here, for $d\rho = |n+1\rangle\langle n+1| - |n\rangle\langle n|$, we have

$$[\mathcal{D}, \pi(d\rho)] = \sqrt{\frac{2}{\theta}} \left(\begin{array}{c|c} 0 & A \\ \hline -A^\dagger & 0 \end{array} \right); \quad \text{where } A = \begin{pmatrix} -\sqrt{n} & 0 & 0 \\ 0 & 2\sqrt{n+1} & 0 \\ 0 & 0 & -\sqrt{n+2} \end{pmatrix} \quad (112)$$

with the rows and columns labeled from top to bottom and left to right respectively by $|n\rangle_+, |n+1\rangle_+, |n+2\rangle_+$ and $|n\rangle_-, |n+1\rangle_-, |n+2\rangle_-$. From this we get the operator norm as

$$\|[\mathcal{D}, \pi(d\rho)]\|_{op} = 2\sqrt{\frac{2(n+1)}{\theta}}. \quad (113)$$

Since $\text{tr}(d\rho)^2 = 2$, we have

$$d(\omega_{n+1}, \omega_n) = |\text{tr}(d\rho a_s)| = \frac{\text{tr}(d\rho)^2}{\|[\mathcal{D}, \pi(d\rho)]\|_{op}} = \sqrt{\frac{\theta}{2(n+1)}}, \quad (114)$$

demonstrating that the result obtained in [7],[1] hold for the “harmonic oscillator” basis, unlike the coherent state of the previous section.

5.2 Distance between finitely separated discrete “harmonic oscillator” states $|n\rangle$ and $|m\rangle$ in the Moyal plane

For the finite case, to compute the distance between $\rho_n \equiv |n\rangle\langle n|$ and $\rho_m \equiv |m\rangle\langle m|$ with the difference between the two integer labels m and n being $|m - n| \geq 2$. We start by writing,

$$\begin{aligned} d(\omega_m, \omega_n) &= \sup_{a \in B} |\text{tr}(\rho_{n+k}a) - \text{tr}(\rho_n a)| \quad ; \quad \text{where } k = m - n \\ &= \sup_{a \in B} |\text{tr}(\rho_{n+k} - \rho_{n+(k-1)} + \rho_{n+(k-1)} - \rho_{n+(k-2)} \cdots + \rho_{n+1} - \rho_n, a)| \\ &= \sup_{a \in B} \left| \text{tr} \left(\sum_{i=1}^k (\rho_{n+i} - \rho_{n+(i-1)}), a \right) \right| \\ &= \sup_{a \in B} \left| \sum_{i=1}^k \text{tr}((\rho_{n+i} - \rho_{n+(i-1)}), a) \right|. \end{aligned}$$

As shown in the infinitesimal case eq (107),

$$\text{tr}((\rho_{n+i} - \rho_{n+(i-1)})a) = \frac{1}{\sqrt{n+i}} \langle n + (i-1) | [b, a] | n + i \rangle.$$

Therefore, proceeding as in the infinitesimal case,

$$d(\omega_m, \omega_n) = \sup_{a \in B} \left| \sum_{i=1}^k \frac{1}{\sqrt{n+i}} \langle n + (i-1) | [b, a] | n + i \rangle \right| \quad (115)$$

$$\leq \sup_{a \in B} \sum_{i=1}^k \frac{1}{\sqrt{n+i}} |\langle n + (i-1) | [b, a] | n + i \rangle| \quad (116)$$

$$\leq \sqrt{\frac{\theta}{2}} \sum_{i=1}^k \frac{1}{\sqrt{n+i}}, \quad (117)$$

by using eq (108) and (69).

To find an optimal element $a_s \in B$ for which the above inequality is saturated, we demand

$$\sum_{i=1}^k \frac{1}{\sqrt{n+i}} \langle n + (i-1) | [b, a_s] | n + i \rangle = \sqrt{\frac{\theta}{2}} \sum_{i=1}^k \frac{1}{\sqrt{n+i}}.$$

Equivalently,

$$\begin{aligned} \left| \sum_{i=1}^k (a_s)_{n+i, n+i} - (a_s)_{n+(i-1), n+(i-1)} \right| &= |(a_s)_{n+k, n+k} - (a_s)_{n, n}| \\ &= \sqrt{\frac{\theta}{2}} \sum_{i=1}^k \frac{1}{\sqrt{n+i}}. \end{aligned}$$

Now if we let $(a_s)_{n+k, n+k} = 0$ it implies $|(a_s)_{n, n}| = \sqrt{\frac{\theta}{2}} \sum_{i=1}^k \frac{1}{\sqrt{n+i}}$. Constructing such an $a_s \in B$ we get,

$$a_s = \sum_{p=0}^{m-1} \left(\sqrt{\frac{\theta}{2}} \sum_{i=1}^{m-p} \frac{1}{\sqrt{p+i}} |p\rangle\langle p| \right), \quad (118)$$

where $m = n + k$. This gives

$$d(\omega_m, \omega_n) = \sqrt{\frac{\theta}{2}} \sum_{i=1}^{m-n} \frac{1}{\sqrt{n+i}}. \quad (119)$$

From the above equation it is also seen that for the “harmonic oscillator” basis

$$d(\omega_m, \omega_n) = d(\omega_m, \omega_l) + d(\omega_l, \omega_n) \quad \text{for } n \leq l \leq m, \quad (120)$$

reproducing the result of [7].

Finally note that a_s (118) is no longer proportional to $\Delta\rho = \rho_m - \rho_n = |m\rangle\langle m| - |n\rangle\langle n|$ unlike (111). Consequently, the distance computed here (119) will exceed the lower bound (42) and $\Delta\rho_\perp$ contributes non-trivially in (55).

6 Fuzzy Sphere

We approach the problem of the fuzzy sphere in quite the same way as the Moyal plane. There are, however, some fundamental differences between these cases and we will comment on these as we proceed. To begin with, we shall first try to find the distance in the discrete basis and later we will look at the continuous coherent state basis. As will be seen in the subsequent discussion, it is convenient to adopt different techniques for these two cases, namely we need to use the Dirac operator eigen-spinors in the latter case.

6.1 Distance Between Discrete States

We begin with a particular fuzzy sphere, corresponding to a particular n . The discrete set of basis are indexed by n_3 as $|n, n_3\rangle$ or just $|n_3\rangle$ in an abbreviated form, where the index ‘ n ’ is suppressed. We shall rather use a subscript ‘ n ’ to denote the distance function $d_n(\omega, \omega')$ between a pair of states ω and ω' .

6.1.1 Infinitesimal Distance

We first compute the distance between the states $\rho_{n_3+1} \equiv |n_3 + 1\rangle\langle n_3 + 1|$ and $\rho_{n_3} \equiv |n_3\rangle\langle n_3|$ (this being the “infinitesimal separation” as far as discrete basis is concerned). Similar to the Moyal case, we start with

$$d_n(\omega_{n_3+1}, \omega_{n_3}) = \sup_{a \in B} |\text{tr}(\rho_{n_3+1} a) - \text{tr}(\rho_{n_3} a)|. \quad (121)$$

Then,

$$\begin{aligned} d_n(\omega_{n_3+1}, \omega_{n_3}) &= \sup_{a \in B} |\langle n_3 | \frac{J_- a J_+}{\sqrt{n(n+1) - n_3(n_3+1)}} | n_3 \rangle - \langle n_3 | a | n_3 \rangle| \\ &= \sup_{a \in B} \frac{1}{\sqrt{n(n+1) - n_3(n_3+1)}} |\langle n_3 | [J_-, a] | n_3 + 1 \rangle|. \end{aligned}$$

Again invoking Bessel’s inequality (108), we can write

$$d_n(\omega_{n_3+1}, \omega_{n_3}) \leq \frac{\|[J_-, a]\|_{op}}{\sqrt{n(n+1) - n_3(n_3+1)}} = \frac{\|[J_+, a]\|_{op}}{\sqrt{n(n+1) - n_3(n_3+1)}} \leq \frac{r_n}{\sqrt{n(n+1) - n_3(n_3+1)}}, \quad (122)$$

where we have made use of the inequality (239), as proved in appendix 8, where for $a \in B$, we have

$$\|[J_-, a]\|_{op} = \|[J_+, a]\|_{op} \leq r_n; \quad r_n = \lambda \sqrt{n(n+1)}. \quad (123)$$

Like in the case of the Moyal plane, we look for an optimal element i.e. an algebra element saturating the upper bound in (122), so that it can be identified as the distance. However, as mentioned before, the optimal element may not be unique. Here, we provide two such optimal elements which saturate the above inequality. We try with the form corresponding to the lower bound (42):

$$a_s = \frac{d\rho}{\|[D, d\rho]\|_{op}} \quad \text{where} \quad d\rho = |n_3 + 1\rangle\langle n_3 + 1| - |n_3\rangle\langle n_3|. \quad (124)$$

The operator norm $\|[D, \pi(d\rho)]\|_{op}$ can now be computed using the Dirac operator eigen-spinor basis (31) as

$$[D, \pi(d\rho)] = \frac{1}{r_n} \begin{pmatrix} 0 & A \\ -A^\dagger & 0 \end{pmatrix}, \quad (125)$$

where

$$A = \begin{pmatrix} -\sqrt{n(n+1) - n_3(n_3-1)} & 0 & 0 \\ 0 & 2\sqrt{n(n+1) - n_3(n_3+1)} & 0 \\ 0 & 0 & -\sqrt{n(n+1) - (n_3+1)(n_3+2)} \end{pmatrix} \quad (126)$$

with the rows and columns labeled from top to bottom and left to right respectively by $|n, n_3 - 1\rangle_+$, $|n, n_3\rangle_+$, $|n, n_3 + 1\rangle_+$ and $|n, n_3 - 1\rangle_-$, $|n, n_3\rangle_-$, $|n, n_3 + 1\rangle_-$. From this we get the operator norm as

$$\|[D, \pi(d\rho)]\|_{op} = \frac{2}{r_n} \sqrt{n(n+1) - n_3(n_3+1)}. \quad (127)$$

Again as $\text{tr}(d\rho)^2 = 2$, we can readily compute this infinitesimal distance to get,

$$d(\omega_{n_3+1}, \omega_{n_3}) = |\text{tr}(d\rho a_s)| = \frac{\text{tr}(d\rho)^2}{\|[D, \pi(d\rho)]\|_{op}} = \frac{r_n}{\sqrt{n(n+1) - n_3(n_3+1)}}. \quad (128)$$

There is yet another optimal element given by

$$a_s = \frac{r_n}{\sqrt{n(n+1) - n_3(n_3+1)}} |n_3+1\rangle\langle n_3+1|. \quad (129)$$

For both these elements, the "infinitesimal distance" is the upper bound itself. Furthermore it also coincides with the lower bound (42). Thus,

$$d_n(\omega_{n_3+1}, \omega_{n_3}) = \frac{\lambda\sqrt{(n(n+1))}}{\sqrt{n(n+1) - n_3(n_3+1)}}. \quad (130)$$

This reproduces the result of [12, 4].

6.1.2 Finite Distance

For the finite case, we try to compute the distance between the states $\rho_{n_3} \equiv |n_3\rangle\langle n_3|$ and $\rho_{m_3} \equiv |m_3\rangle\langle m_3|$ with $|m_3 - n_3| \geq 2$ and $-n \leq m_3, n_3 \leq n$. Again, adopting the same technique as in the Moyal plane, we write

$$\begin{aligned} d_n(\omega_{m_3}, \omega_{n_3}) &= \sup_{a \in B} |\text{tr}(\rho_{n_3+k}a) - \text{tr}(\rho_{n_3}a)| \quad ; \quad \text{where } k = m_3 - n_3 \\ &= \sup_{a \in B} \left| \sum_{i=1}^k \text{tr}((\rho_{n_3+i} - \rho_{n_3+(i-1)}), a) \right| \\ &\leq \sup_{a \in B} \sum_{i=1}^k \frac{|\langle n_3 + (i-1) | [J_-, a] | n_3 + i \rangle|}{\sqrt{n(n+1) - (n_3+i)(n_3+i-1)}} \\ &\leq \sum_{i=1}^k \frac{r_n}{\sqrt{n(n+1) - (n_3+i)(n_3+i-1)}}. \end{aligned}$$

It can be easily verified that the element $a_s \in B$, for which the above inequality is saturated is given by

$$a_s = \sum_{p=n_3}^{m_3-1} \left(\sum_{i=1}^{m_3-p} \frac{r_n}{\sqrt{n(n+1) - (p+i)(p+i-1)}} |p\rangle\langle p| \right), \quad (131)$$

which gives

$$d_n(\omega_{m_3}, \omega_{n_3}) = \sum_{i=1}^k \frac{r_n}{\sqrt{n(n+1) - (n_3+i)(n_3+i-1)}}. \quad (132)$$

From the above equation it is evident that for the discrete basis,

$$d_n(\omega_{m_3}, \omega_{n_3}) = d_n(\omega_{m_3}, \omega_{l_3}) + d_n(\omega_{l_3}, \omega_{n_3}) \quad \text{for } n_3 \leq l_3 \leq m_3 \quad (133)$$

i.e. the distance between finitely separated states are additive and they saturate the triangle inequality for the fuzzy sphere, much like in the case of the Moyal plane. In particular the distance between the north pole (N), denoted by $\omega_n = |n\rangle\langle n|$ and south pole (S), denoted by $\omega_{-n} = |-n\rangle\langle -n|$ is given by

$$d_n(N, S) = d_n(\omega_n, \omega_{-n}) = \sum_{k=1}^{2n} \frac{r_n}{\sqrt{k(2n+1-k)}}, \quad \forall n. \quad (134)$$

Since both the discrete states ω_n and ω_{-n} , representing north and south poles are also coherent states, we should be able to reproduce the same results in our coherent state calculations, to be taken up in the next subsection. Furthermore, since the $n = 1/2$ case corresponds to maximal non-commutativity let us just write down the distance between the north (N) and south poles (S) for the lowest three cases $n = 1/2$, $n = 1$ and $n = 3/2$ respectively - as special cases. They are given by

$$d_{1/2}(N, S) = r_{1/2} \quad ; \quad d_1(N, S) = \sqrt{2} r_1 \quad ; \quad d_{3/2}(N, S) = \left(\frac{1}{2} + \frac{2\sqrt{3}}{3} \right) r_{3/2} = 1.6547 r_{3/2}. \quad (135)$$

The coefficients in front of $r_{1/2}$, r_1 and $r_{3/2}$ here indicates that they are highly deformed spaces and the corresponding distances are way below the corresponding commutative spheres $\pi r_{1/2}$, πr_1 and $\pi r_{3/2}$ respectively. This is just indicative of the fact that none of the fuzzy spheres with fixed n allows one to define a geodesic in the conventional sense. We have more to say on this in the following subsections. However, one can expect the results to match with the commutative ones in the large n limit so that the distance as given in (134), in the limit $n \rightarrow \infty$, should match asymptotically with πr_n , which is the geodesic distance between north and south pole for a commutative sphere.

To implement the commutative limit, we take $k/n = x_k$ and $\Delta x = x_k - x_{k-1} = 1/n$ as the increment such that $\Delta x \rightarrow 0$ as $n \rightarrow \infty$. Then we can rewrite

$$\begin{aligned} \lim_{n \rightarrow \infty} \frac{d_n(N, S)}{r_n} &= \lim_{n \rightarrow \infty} \sum_{k=1}^{2n} \frac{1}{\sqrt{k(2n+1-k)}} \\ &= \lim_{n \rightarrow \infty} \sum_{k=1}^{2n} \frac{\frac{1}{n}}{\sqrt{\frac{k}{n}(2 + \frac{1}{n} - \frac{k}{n})}} = \lim_{\Delta x \rightarrow 0} \sum_{x=x_1}^{x_{2n}=2} \frac{\Delta x}{\sqrt{x_k(2 + \Delta x - x_k)}} \rightarrow \int_0^2 \frac{dx}{\sqrt{x(2-x)}} \\ &= 2 \int_0^1 \frac{dt}{\sqrt{1-t^2}} = \pi, \end{aligned} \quad (136)$$

where we have set $x = 1 - t$ to obtain the last integral.

6.2 Upper bound of the distance between coherent states

Let us proceed along the same line for the Moyal plane. The Perelomov coherent states for the fuzzy sphere is constructed by [11]

$$|z\rangle = e^{-iJ_2\theta}|n, n\rangle = U_F(z, \langle z|)|n\rangle \quad (137)$$

where, $\frac{\theta}{2} = \tan^{-1}|z|$ and $|n\rangle$ is the abbreviation for $|n, n\rangle$. Note that we have taken for convenience the azimuthal angle $\varphi = 0$. This can be done without loss of generality.

Now for the state ω_z we have,

$$\begin{aligned} \omega_z(a) &= \text{tr}(\rho_z a) = \text{tr}\left(U_F(z, \bar{z})|n\rangle\langle n|U_F^\dagger(z, \bar{z})a\right) \\ &= \langle n|(U_F^\dagger(z, \bar{z})aU_F(z, \bar{z}))|n\rangle; \quad a \in \mathcal{H}_q \equiv \mathcal{A}. \end{aligned} \quad (138)$$

To calculate the upper bound, we write the distance as

$$d(\omega_z, \omega_0) = \sup_{a \in B} |\langle n|(U_F^\dagger(z, \langle z|)aU_F(z, \langle z|))|n\rangle - \langle n|a|n\rangle|. \quad (139)$$

We again construct the one-parameter family $W(t) = \omega_{zt}(a) = \text{tr}(\rho_{zt}a)$, with $t \in [0, 1]$ being a real parameter and $a = a^\dagger$. We then have for pair of states ω and ω' ,

$$|\omega(a) - \omega'(a)| = \left| \int_0^1 \frac{dW(t)}{dt} dt \right| \leq \int_0^1 \left| \frac{dW(t)}{dt} \right| dt. \quad (140)$$

Here

$$\begin{aligned} (U_F^\dagger(z, \bar{z})aU_F(z, \bar{z})) &= \exp(G)a \exp(-G) \\ &= a + [G, a] + \frac{1}{2!}[G, [G, a]] + \frac{1}{3!}[G, [G, [G, a]]] + \dots, \end{aligned} \quad (141)$$

where $G = \frac{\theta}{2}(J_+ - J_-)$, $|\alpha| = \tan^{-1}|z|$ and

$$\left| \frac{dW(t)}{dt} \right| = \left(\frac{|z|dt}{1 + |z|^2 t^2} \right) \left| \omega_{zt} \left(\frac{[G, a]}{|\alpha|} \right) \right|. \quad (142)$$

Since [see appendix 8, (244)]

$$\frac{1}{r_n} \|[J_+, a]\|_{\text{op}} \leq \|[\mathcal{D}, \pi(a)]\|_{\text{op}} \quad \text{and} \quad \frac{1}{r_n} \|[J_-, a]\|_{\text{op}} \leq \|[\mathcal{D}, \pi(a)]\|_{\text{op}}$$

for $a \in B$, this implies

$$\|[J_+, a]\|_{\text{op}} \leq \lambda \sqrt{n(n+1)} \quad \text{and} \quad \|[J_-, a]\|_{\text{op}} \leq \lambda \sqrt{n(n+1)}.$$

Using the Cauchy-Schwartz inequality we get

$$\begin{aligned} \left| \omega_{zt} \left(\frac{[G, a]}{|\alpha|} \right) \right| &= |\omega_{zt}([J_+, a]) - \omega_{zt}([J_-, a])| \\ &\leq \sqrt{2} \sqrt{|\omega_{zt}([J_+, a])|^2 + |\omega_{zt}([J_-, a])|^2} \\ &\leq \sqrt{2} \sqrt{\|[J_+, a]\|_{\text{op}}^2 + \|[J_-, a]\|_{\text{op}}^2} \\ &\leq 2r_n. \end{aligned}$$

Thus we get from (140) and (142),

$$\begin{aligned} |\omega_z(a) - \omega_0(a)| &\leq \int_0^1 \left| \frac{dW(t)}{dt} \right| dt = \int_0^1 \left(\frac{|z|dt}{1 + |z|^2 t^2} \right) \left| \omega_{zt} \left(\frac{[G, a]}{|\alpha|} \right) \right| \\ &\leq (2r_n) \int_0^1 \left(\frac{|z|dt}{1 + |z|^2 t^2} \right) = 2r_n \tan^{-1} |z| = r_n \theta. \end{aligned} \quad (143)$$

Therefore the upper bound of the Connes distance on the fuzzy sphere is actually the geodesic distance on the commutative sphere

$$d(\omega_z, \omega_0) = \sup_{a \in B} |\omega_z(a) - \omega_0(a)| \leq 2r \tan^{-1} |z| = r\theta. \quad (144)$$

The stark difference with the Moyal plane is that we cannot find any algebra element saturating this inequality (144), not even through a sequence or through projections. This limit is actually the distance on a commutative sphere and is reached only for the commutative limit, $n \rightarrow \infty$ as we have shown earlier. This implies that for any finite n representation, the distance between two points on the fuzzy sphere is less than the geodesic distance for a commutative sphere (see (135), for example) and the distance does not follow the conventional ‘geodesic’ path as we know it. Indeed, we will show that for $n = 1/2$, the distance actually corresponds to half of the chordal distance between a pair of points on the surface of the sphere or more precisely between the associated pure states and interpolated by a one parameter family of mixed states. Only in the limit $n \rightarrow \infty$ this slowly deforms to become the great circle path on the surface.

6.3 Ball condition in the eigen-spinor basis

For the calculation of distances for coherent states or more precisely the operator-norm occurring in the ball condition (33), we now make use of the eigen-spinors (31) of the Dirac operator (30). We will first sketch the outline of the algorithm. One can calculate in a straightforward manner (at least in principle) the commutator $[\mathcal{D}, \pi(a)]$ in the above-mentioned eigen-spinor basis to obtain

$$[\mathcal{D}, \pi(a)] = \frac{1}{r_n} \left(\begin{array}{c|c} 0_{(2n+2) \times (2n+2)} & A_{(2n+2) \times 2n} \\ \hline -A_{2n \times (2n+2)}^\dagger & 0_{(2n) \times (2n)} \end{array} \right), \quad (145)$$

where we denote the non-vanishing rectangular matrices by A and A^\dagger as

$$\begin{aligned} A_{(2n+2) \times 2n} &= (2n+1)_+ \langle \langle n, n_3 | \pi(a) | n, n'_3 \rangle \rangle_- \Rightarrow + \langle \langle n, n_3 | [\mathcal{D}, \pi(a)] | n, n'_3 \rangle \rangle_- \equiv \frac{1}{r_n} A_{(2n+2) \times 2n} \\ A_{2n \times (2n+2)}^\dagger &= (2n+1)_- \langle \langle n, n'_3 | \pi(a) | n, n_3 \rangle \rangle_+ \Rightarrow - \langle \langle n, n'_3 | [\mathcal{D}, \pi(a)] | n, n_3 \rangle \rangle_+ \equiv -\frac{1}{r_n} A_{2n \times (2n+2)}^\dagger \end{aligned} \quad (146)$$

with the respective ranges for n_3 and n'_3 given by: $-n-1 \leq n_3 \leq n$ and $n-1 \leq n'_3 \leq n-1$.

The occurrences of rectangular null matrices in the diagonal blocks of (145) stems from the degeneracy of the spectrum of the Dirac operator (see comments below (32)). This yields a block diagonal form for

$$[\mathcal{D}, \pi(a)]^\dagger [\mathcal{D}, \pi(a)] = \frac{1}{r_n^2} \left(\begin{array}{c|c} (AA^\dagger)_{(2n+2) \times (2n+2)} & 0_{(2n+2) \times 2n} \\ \hline 0_{2n \times (2n+2)} & (A^\dagger A)_{2n \times 2n} \end{array} \right) \quad (147)$$

and, from the C^* -algebra, property we have

$$\|[\mathcal{D}, \pi(a)]\|_{\text{op}}^2 = \|[\mathcal{D}, \pi(a)]^\dagger [\mathcal{D}, \pi(a)]\|_{\text{op}} = \frac{1}{r_n^2} \|AA^\dagger\|_{\text{op}} = \frac{1}{r_n^2} \|A^\dagger A\|_{\text{op}}. \quad (148)$$

In what follows we shall make use of (42) to first obtain the lower bound of the infinitesimal distance for a general n representation. This will help us improve the estimate by introducing a suitable transverse part $\Delta\rho_\perp$ in (55). We consider the $n = 1/2$ and $n = 1$ representations separately in the subsequent subsections and try to calculate the finite Connes distance between the ‘north pole’ and some other points represented by appropriate coherent states. We will see that although the revised formula (54) indicates that $\Delta\rho_\perp$ might play a role in the distance calculation for $n = 1/2$ the lower bound will itself correspond to the exact distance, leaving no room for $\Delta\rho_\perp$ to contribute. However, for $n = 1$ it will indeed play an important role in improving our estimation of the lower bound, except for $\theta = \pi$, where again $\Delta\rho_\perp$ will make no contribution.

6.4 Lower Bound for Infinitesimally Separated Coherent States

Following the algorithm as explained in the previous subsection 6.3, we easily find that $d\rho$ is in this case given by

$$d\rho = |dz\rangle\langle dz| - |n\rangle\langle n|. \quad (149)$$

Using the infinitesimal version of (137), this yields

$$d\rho = d\theta \sqrt{\frac{n}{2}} [|n\rangle\langle n-1| + |n-1\rangle\langle n|]. \quad (150)$$

Making use of (146), we get the matrix form in the Dirac eigenbasis for $[\mathcal{D}, \pi(d\rho)]$ as

$$[\mathcal{D}, \pi(d\rho)] \equiv \frac{1}{r_n} \left(\begin{array}{c|c} 0 & A \\ \hline -A^\dagger & 0 \end{array} \right), \quad (151)$$

where

$$A = \begin{pmatrix} d\theta\sqrt{n(n+\frac{1}{2})} & 0 & 0 \\ 0 & -d\theta\sqrt{n(n-\frac{1}{2})} & 0 \\ -d\theta n\sqrt{2} & 0 & 0 \end{pmatrix}. \quad (152)$$

Here rows/columns are labeled from up to down/left to right respectively by $|n\rangle\rangle_+$, $|n-1\rangle\rangle_+$, $|n-2\rangle\rangle_+$ and $|n-1\rangle\rangle_-$, $|n-2\rangle\rangle_-$, $|n-3\rangle\rangle_-$. Subsequently, we get

$$[\mathcal{D}, \pi(d\rho)]^\dagger [\mathcal{D}, \pi(d\rho)] = \frac{1}{r_n^2} \left(\begin{array}{c|c} AA^\dagger & 0 \\ \hline 0 & A^\dagger A \end{array} \right) \quad (153)$$

with

$$A^\dagger A = n(d\theta)^2 \begin{pmatrix} 3n + \frac{1}{2} & 0 & 0 \\ 0 & n - \frac{1}{2} & 0 \\ 0 & 0 & 0 \end{pmatrix}. \quad (154)$$

Since $\|[\mathcal{D}, \pi(d\rho)]^\dagger [\mathcal{D}, \pi(d\rho)]\|_{\text{op}} = \frac{1}{r_n^2} \|A^\dagger A\|_{\text{op}}$, as follows from (147), we have

$$\|[\mathcal{D}, \pi(d\rho)]\|_{\text{op}} = \frac{1}{r_n} \sqrt{\|A^\dagger A\|_{\text{op}}} = \frac{d\theta}{r_n} \sqrt{n(3n + \frac{1}{2})}. \quad (155)$$

Using this, the lower bound (42) comes out to be

$$d(\omega_{z+dz}, \omega_z) \geq \frac{\text{tr}(d\rho^2)}{\|[\mathcal{D}, \pi(d\rho)]\|_{\text{op}}} = r_n d\theta \sqrt{\frac{2n}{6n+1}}. \quad (156)$$

Clearly, for $n = 1/2$ this comes out to be $r_{1/2} \frac{d\theta}{2}$. We show later that it coincides with the correct infinitesimal version of the finite distance for the $n = 1/2$ case, to be computed in the next subsection.

6.5 The $n = 1/2$ fuzzy sphere

Clearly here the algebra element can be taken to be a traceless hermitian 2×2 matrix without loss of generality. The traceless condition stems from the fact that the 2×2 identity matrix $\mathbf{1}_2$ commutes with Dirac operator and therefore does not contribute to the ball condition. One can thus parametrise any generic algebra element ‘ a ’ in terms of a 3-vector $\vec{a} \in \mathbb{R}^3$, by writing

$$a = \vec{a} \cdot \vec{\sigma} \quad (157)$$

where $\vec{\sigma}$ stands for the three Pauli matrices.

This enables us to express all the matrix elements of $[\mathcal{D}, \pi(a)]$ in terms of the coefficients a_i . For any generic pair of states $|m\rangle\rangle_+$ and $|m'\rangle\rangle_-$ we have, by making use of the general framework sketched in section (6.3), the matrix element,

$$+\langle\langle m | [\mathcal{D}, \pi(a)] | m' \rangle\rangle_- = \frac{2}{r_{1/2}} + \langle\langle m | \pi(a) | m' \rangle\rangle_-, \quad (158)$$

where m takes values $-\frac{3}{2}, -\frac{1}{2}, \frac{1}{2}$ and $m' = -\frac{1}{2}$. On explicit computation, one finds the following matrix elements for the commutator:

$$+\langle\langle -\frac{3}{2} | \pi(a) | -\frac{1}{2} \rangle\rangle_- = \frac{1}{\sqrt{2}}(a_1 + ia_2); \quad +\langle\langle -\frac{1}{2} | \pi(a) | -\frac{1}{2} \rangle\rangle_- = a_3; \quad +\langle\langle \frac{1}{2} | \pi(a) | -\frac{1}{2} \rangle\rangle_- = -\frac{1}{\sqrt{2}}(a_1 - ia_2) \quad (159)$$

so that the final form of the commutator matrix (146) in this case can be written as

$$[\mathcal{D}, \pi(a)] \equiv \frac{1}{r_{1/2}} \left(\begin{array}{c|c} 0_{3 \times 3} & A_{3 \times 1} \\ \hline -A_{1 \times 3}^\dagger & 0 \end{array} \right), \quad \text{where } A_{3 \times 1} = 2 + \langle\langle m | [\mathcal{D}, \pi(a)] | m' \rangle\rangle_- = \begin{pmatrix} \sqrt{2}(a_1 + ia_2) \\ 2a_3 \\ -\sqrt{2}(a_1 - ia_2) \end{pmatrix}. \quad (160)$$

Finally,

$$[\mathcal{D}, \pi(a)]^\dagger [\mathcal{D}, \pi(a)] = \frac{1}{r_{1/2}^2} \left(\begin{array}{c|c} AA^\dagger & 0 \\ \hline 0 & A^\dagger A \end{array} \right). \quad (161)$$

Since $\|A^\dagger A\|_{\text{op}} = \|AA^\dagger\|_{\text{op}} = r_{1/2}^2 \|[\mathcal{D}, \pi(a)]^\dagger [\mathcal{D}, \pi(a)]\|_{\text{op}}$ and $A^\dagger A$ is just a number, we have

$$\|[\mathcal{D}, \pi(a)]^\dagger [\mathcal{D}, \pi(a)]\|_{\text{op}} = \frac{1}{r_{1/2}^2} \|A^\dagger A\|_{\text{op}} = \frac{4}{r_{1/2}^2} (a_1^2 + a_2^2 + a_3^2) = \frac{4}{r_{1/2}^2} |\vec{a}|^2. \quad (162)$$

Thus, the ball condition reduces to

$$\|[\mathcal{D}, \pi(a)]\|_{\text{op}} = \frac{2}{r_{1/2}} |\vec{a}| \leq 1. \quad (163)$$

Equivalently, and interestingly, this yields a solid ball in \mathbb{R}^3 :

$$|\vec{a}| \leq \frac{r_{1/2}}{2}. \quad (164)$$

We have mentioned that from the symmetry of the space, we can choose any point as the North pole of the sphere. Here, for $n = \frac{1}{2}$, all pure states are coherent states such that we can parametrise a pair of generalized points (pure states) as

$$1. \rho_N = \rho_{\theta=0} = \begin{pmatrix} 1 & \\ & 0 \end{pmatrix} \begin{pmatrix} 1 & 0 \\ 0 & 0 \end{pmatrix} = \begin{pmatrix} 1 & 0 \\ 0 & 0 \end{pmatrix},$$

$$2. \rho_P = \rho_{\theta_0} = U(\theta_0) \begin{pmatrix} 1 & \\ & 0 \end{pmatrix} U^\dagger(\theta_0) = \frac{1}{2} \begin{pmatrix} 1 + \cos \theta_0 & \sin \theta_0 \\ \sin \theta_0 & 1 - \cos \theta_0 \end{pmatrix}, \quad U(\theta_0) = \begin{pmatrix} \cos \frac{\theta_0}{2} & -\sin \frac{\theta_0}{2} \\ \sin \frac{\theta_0}{2} & \cos \frac{\theta_0}{2} \end{pmatrix} \in SU(2),$$

where in general $\omega_\theta(a) = \text{tr}(\rho_\theta a)$. We define $\Delta\rho = \rho_{\theta_0} - \rho_0$. Being a traceless hermitian matrix, this too can be expanded like (157):

$$\Delta\rho = \vec{\Delta\rho} \cdot \vec{\sigma}, \quad \text{where } (\Delta\rho)_1 = \frac{\sin \theta_0}{2}; \quad (\Delta\rho)_2 = 0; \quad (\Delta\rho)_3 = \frac{-1 + \cos \theta_0}{2}. \quad (165)$$

With this, we have

$$|\omega_{\theta_0}(a) - \omega_0(a)| = |\text{tr}_{\mathcal{H}_n}(\Delta\rho a)| = |2\vec{a} \cdot \vec{\Delta\rho}|. \quad (166)$$

Since both \vec{a} and $\vec{\Delta\rho} \in \mathbb{R}^3$, the supremum of $|\vec{a} \cdot \vec{\Delta\rho}|$ will be attained when \vec{a} and $\vec{\Delta\rho}$ are parallel or anti-parallel to each other. Thus, with the ball condition (164) and (165), we get the spectral distance between a pair of pure states ρ_0 and ρ_{θ_0} as

$$d_{\frac{1}{2}}(\omega_{\theta_0}, \omega_0) = \sup_{|\vec{a}| \leq \frac{r_{1/2}}{2}} |\omega_{\theta_0}(a) - \omega_0(a)| = r_{\frac{1}{2}} \sqrt{(\Delta\rho)_1^2 + (\Delta\rho)_3^2} = r_{\frac{1}{2}} \sin \frac{\theta_0}{2}. \quad (167)$$

This is just half of the chordal distance connecting NP , reproducing the result of [12]. Since the supremum is attained here where \vec{a} and $\vec{\Delta\rho}$ are parallel, the distance function just corresponds to the lower bound (42). The corresponding infinitesimal distance $d(\omega_{d\theta}, \omega_0) = \frac{1}{2} r_{\frac{1}{2}} d\theta$ can easily be seen to match exactly with (156), by setting $n = \frac{1}{2}$.

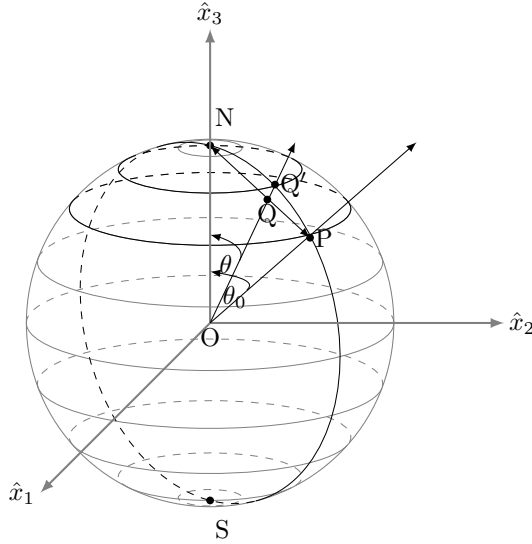


Figure 1: Space of Perelomov's $SU(2)$ coherent states for $n = \frac{1}{2}$.

Let us now consider a family of mixed states (as shown in the figure 1). A generic mixed state ρ_Q , represented by the point Q on the chord NP inside the sphere, is obtained from the following convex sum:

$$\rho_t = (1-t)\rho_N + t\rho_P = \frac{1}{2} \begin{pmatrix} 2-t(1-\cos \theta_0) & t \sin \theta_0 \\ t \sin \theta_0 & t(1-\cos \theta_0) \end{pmatrix}; \quad 0 \leq t \leq 1. \quad (168)$$

Clearly, $\rho_0 = \rho_N$ and $\rho_1 = \rho_P$. Introducing $(\Delta\rho)_{QN} = \rho_t - \rho_N$ and $(\Delta\rho)_{PN} = \rho_P - \rho_t$ such that

$$\begin{aligned} ((\Delta\rho)_{QN})_1 &= \frac{t \sin \theta_0}{2}, \quad ((\Delta\rho)_{QN})_2 = 0, \quad ((\Delta\rho)_{QN})_3 = -\frac{t(1-\cos \theta_0)}{2} \\ ((\Delta\rho)_{PN})_1 &= \frac{(1-t) \sin \theta_0}{2}, \quad ((\Delta\rho)_{PN})_2 = 0, \quad ((\Delta\rho)_{PN})_3 = -\frac{(1-t)(1-\cos \theta_0)}{2}, \end{aligned}$$

we get the spectral distances between the mixed state ω_t and ω_N and ω_P respectively as

$$d(\omega_t, \omega_N) = t r_{\frac{1}{2}} \sin \frac{\theta_0}{2} \quad \text{and} \quad d(\omega_P, \omega_t) = (1-t) r_{\frac{1}{2}} \sin \frac{\theta_0}{2}. \quad (169)$$

The fact that the distance of this mixed state ω_t from the extremal, pure states ω_N and ω_P are proportional to the parameters t and $(1-t)$ respectively indicates that we can identify a unique pure state Q' (see fig 1) nearest to a given mixed state Q just by extending the straight line OQ from the center O to the surface of the sphere. This distance can therefore be used alternatively to characterize the ‘mixedness’ of a spin-1/2 system. Further, we have

$$d(\omega_{\theta_0}, \omega_0) = d(\omega_P, \omega_N) = d(\omega_P, \omega_t) + d(\omega_t, \omega_N). \quad (170)$$

This is just analogous to (105), except that the intermediate state ω_t is not pure. This chord cannot therefore be identified as a conventional geodesic. This same family can be parametrised alternatively [12] as

$$\rho_\theta = \frac{1}{2}(\mathbb{1}_2 + \vec{\sigma} \cdot \vec{n}_\theta) = \frac{1}{2} \begin{pmatrix} 1 + |\vec{n}_\theta| \cos \theta & |\vec{n}_\theta| \sin \theta \\ |\vec{n}_\theta| \sin \theta & 1 - |\vec{n}_\theta| \cos \theta \end{pmatrix}, \quad (171)$$

where $|\vec{n}_\theta|$ is the magnitude the vector \vec{n}_θ parametrising each of the mixed states between the two extremal pure states and is given by

$$\vec{n}_\theta = |\vec{n}_\theta| (\sin \theta, 0, \cos \theta). \quad (172)$$

Clearly, $|\vec{n}_\theta|$ is strictly less than 1 : $|\vec{n}_\theta| < 1$ except for the extremal pure states at $\theta = 0$ and $\theta = \theta_0$. Further the mixed state ρ_θ for the open interval $(0, \theta_0)$ represents a point Q in the chord connecting the north pole $N(\theta = 0)$ and point $P(\theta = \theta_0)$, and therefore lies in the interior of the sphere. Indeed, these two different parameters t and θ for the same state can be related by setting $\rho_\theta = \rho_t$, to get

$$t = \frac{1 - |\vec{n}_\theta| \cos \theta}{1 - \cos \theta_0} = \frac{|\vec{n}_\theta| \sin \theta}{\sin \theta_0} \Rightarrow |\vec{n}_\theta| = \frac{\cos(\frac{\theta_0}{2})}{\cos(\theta - \frac{\theta_0}{2})} \equiv \frac{OQ}{r_{1/2}}, \quad ON = OP = r_{1/2}. \quad (173)$$

Thus, we can recast the spectral distance between a mixed state represented by ρ_θ and the pure states ρ_N and ρ_P (169) respectively as

$$d(\omega_\theta, \omega_N) = \frac{r_{\frac{1}{2}} \sin \theta}{2 \cos(\theta - \frac{\theta_0}{2})} \quad \text{and} \quad d(\omega_P, \omega_\theta) = \frac{r_{\frac{1}{2}} \sin(\theta_0 - \theta)}{2 \cos(\theta - \frac{\theta_0}{2})}. \quad (174)$$

For the case $\theta = \theta_0$, we get $d(\omega_{\theta_0}, \omega_N) = r_{\frac{1}{2}} \sin \frac{\theta_0}{2}$ and $d(\omega_P, \omega_{\theta_0}) = 0$.

Finally, we can also obtain the distance between pure states represented by $\rho_\pi = \begin{pmatrix} 0 & 0 \\ 0 & 1 \end{pmatrix}$ (South pole S) and ρ_{θ_0} (P) as

$$d(\rho_\pi, \rho_{\theta_0}) = r_{\frac{1}{2}} \cos \frac{\theta}{2}. \quad (175)$$

This implies that

$$[d(\rho_0, \rho_{\theta_0})]^2 + [d(\rho_\pi, \rho_{\theta_0})]^2 = r_{1/2}^2. \quad (176)$$

That is, the Pythagoras identity ($NP^2 + SP^2 = NS^2$) is obeyed. All these features, however, will not persist for higher ‘ n ’, as we shall see.

6.6 Analogy with CP^1 model and mixed states

For the spectral triple (35), the space of vector states is CP^1 [22]. We can parametrize a pair of CP^1 -doublets, associated to the pair of points lying in the same latitude (i.e. the same polar angle θ) [4] as

$$\chi = \begin{pmatrix} \cos \frac{\theta}{2} \\ \sin \frac{\theta}{2} e^{i\phi} \end{pmatrix} \longrightarrow \rho = \chi \chi^\dagger; \quad \chi' = \begin{pmatrix} \cos \frac{\theta}{2} \\ \sin \frac{\theta}{2} e^{i\phi'} \end{pmatrix} \longrightarrow \rho' = \chi' \chi'^\dagger. \quad (177)$$

Here, the spectral distance between these two points is obtained as

$$d(\omega_{\rho'}, \omega_\rho) = \frac{2 \sin \theta}{|D_1 - D_2|} \left| \sin \left(\frac{\phi - \phi'}{2} \right) \right|, \quad (178)$$

which corresponds to the distance measured along the chord connecting the pair of points (θ, ϕ) and (θ, ϕ') , at the same latitude θ .

Now, let us define a family of mixed states out of this pair of pure states ρ and ρ' in an analogous way as for the $n = 1/2$ representation (168):

$$\rho_t = (1-t)\rho + t\rho'. \quad (179)$$

Similarly, we obtain the distances between the mixed state ρ_t and the corresponding pure states ρ representing the point (θ, ϕ) and ρ' representing (θ, ϕ') as

$$d(\omega_{\rho_t}, \omega_\rho) = t \frac{2 \sin \theta}{|D_1 - D_2|} \left| \sin \left(\frac{\phi - \phi'}{2} \right) \right|; \quad \text{and} \quad d(\omega_{\rho'}, \omega_{\rho_t}) = (1-t) \frac{2 \sin \theta}{|D_1 - D_2|} \left| \sin \left(\frac{\phi - \phi'}{2} \right) \right|. \quad (180)$$

Clearly, we have

$$d(\omega_{\rho'}, \omega_\rho) = d(\omega_{\rho'}, \omega_{\rho_t}) + d(\omega_{\rho_t}, \omega_\rho). \quad (181)$$

6.7 The $n = 1$ fuzzy sphere

The computation for $n = 1$, presented in this section, is expected to be much more complicated than the $n = \frac{1}{2}$ case, simply because we expect deviations from the straight line chord and the associated Pythagoras relation (176) to show here, while in the extreme $n \rightarrow \infty$ limit this should merge with the great circle of the commutative sphere. It is obvious that one needs to consider the entire $su(3)$ algebra, which in the 3×3 matrix representation are spanned by 8 traceless Gell-Mann matrices, as in (157). The identity matrix is not considered, since it commutes with the Dirac operator and hence will make no contribution to the operator norm $\|[\mathcal{D}, \pi(a)]\|_{op}$. We therefore consider the algebra element a to be traceless throughout this section. It is quite tempting to start directly by identifying the algebra element a as a linear combination of the Gell-Mann matrices. This algebra element with some extra restrictions provide us with a simple expression of the distance using (33), which we then corroborate with a more rigorous calculation using (54). The role of $\Delta\rho_\perp$ turns out to be very important in (54) and (55) for the $n = 1$ fuzzy sphere and we employ the most general form of $\Delta\rho_\perp$ possible to improve the estimate of the spectral distance as best as we can from the lower bound (42) i.e. $\kappa = 0$ case in (54). The determination of an exact value, even with the help of *Mathematica*, remains a daunting task.

6.7.1 Ball condition, general strategy to compute infimum and general form of $\Delta\rho$

To begin with the $n = 1$ case we first proceed in the same way as in section 6.5 to obtain, using (146),

$$+\langle\langle n_3 | [\mathcal{D}, \pi(a)] | n'_3 \rangle\rangle_- = \frac{3}{r_1} + \langle\langle n_3 | \pi(a) | n'_3 \rangle\rangle_- \quad \text{and} \quad -\langle\langle n'_3 | [\mathcal{D}, \pi(a)] | n_3 \rangle\rangle_+ = -\frac{3}{r_1} - \langle\langle n'_3 | \pi(a) | n_3 \rangle\rangle_+, \quad (182)$$

where the ranges of n_3, n'_3 are respectively given by $-2 \leq n_3 \leq 1$ and $-1 \leq n'_3 \leq 0$ so that with the diagonal representation the commutator $[\mathcal{D}, \pi(a)]$ takes the following off-block diagonal form:

$$[\mathcal{D}, \pi(a)] = \frac{1}{r_1} \left(\begin{array}{c|c} 0_{4 \times 4} & A_{4 \times 2} \\ \hline -A_{2 \times 4}^\dagger & 0_{2 \times 2} \end{array} \right), \quad (183)$$

where the rectangular matrices $A_{4 \times 2}$ and $A_{2 \times 4}^\dagger$ are given by

$$A_{4 \times 2} = \begin{pmatrix} -\sqrt{3}a_{1,0} & -\sqrt{6}a_{1,-1} \\ \sqrt{2}(a_{1,1} - a_{0,0}) & (a_{1,0} - 2a_{0,-1}) \\ (2a_{0,1} - a_{-1,0}) & \sqrt{2}(a_{0,0} - a_{-1,-1}) \\ \sqrt{6}a_{-1,1} & \sqrt{3}a_{-1,0} \end{pmatrix}, \quad (184)$$

$$A_{2 \times 4}^\dagger = \begin{pmatrix} -\sqrt{3}a_{0,1} & \sqrt{2}(a_{1,1} - a_{0,0}) & (2a_{1,0} - a_{0,-1}) & \sqrt{6}a_{1,-1} \\ -\sqrt{6}a_{-1,1} & (a_{0,1} - 2a_{-1,0}) & \sqrt{2}(a_{0,0} - a_{-1,-1}) & \sqrt{3}a_{0,-1} \end{pmatrix}. \quad (185)$$

Note that here $a_{m,n}$ are the usual matrix elements $\langle m | a | n \rangle$, with $m, n \in \{1, 0, -1\}$. Using the above result for $[\mathcal{D}, \pi(a)]$ we readily obtain:

$$[\mathcal{D}, \pi(d\rho)]^\dagger [\mathcal{D}, \pi(d\rho)] = \frac{1}{r_1^2} \left(\begin{array}{c|c} (AA^\dagger)_{4 \times 4} & 0_{4 \times 2} \\ \hline 0_{2 \times 4} & (A^\dagger A)_{2 \times 2} \end{array} \right). \quad (186)$$

By exploiting the properties of the operator norm one has the freedom to choose between the two block-diagonal square matrices as $\frac{1}{r_1^2} \|AA^\dagger\|_{op} = \frac{1}{r_1^2} \|A^\dagger A\|_{op} = \|[\mathcal{D}, \pi(a)]^\dagger [\mathcal{D}, \pi(a)]\|_{op} = \|[\mathcal{D}, \pi(a)]\|_{op}^2$. We choose to work with the more convenient one i.e. the 2×2 matrix $(A^\dagger A)_{2 \times 2}$ which turns out to be

$$M := (A^\dagger A)_{2 \times 2} = \begin{pmatrix} M_{11} & M_{12} \\ M_{12}^* & M_{22} \end{pmatrix}, \quad (187)$$

where

$$\begin{aligned} M_{11} &= 3|a_{0,1}|^2 + 2(a_{0,0} - a_{1,1})^2 + |a_{0,-1} - 2a_{1,0}|^2 + 6|a_{1,-1}|^2, \\ M_{22} &= 3|a_{0,-1}|^2 + 2(a_{0,0} - a_{-1,-1})^2 + |a_{1,0} - 2a_{0,-1}|^2 + 6|a_{1,-1}|^2, \\ M_{12} &= \sqrt{2} \{ 3a_{1,-1}(a_{0,1} + a_{-1,0}) + (a_{0,0} - a_{1,1})(2a_{0,-1} - a_{1,0}) + (a_{0,0} - a_{-1,-1})(2a_{1,0} - a_{0,-1}) \}. \end{aligned}$$

This matrix has two eigenvalues E_\pm :

$$E_\pm := \frac{1}{2} \left(P \pm \sqrt{Q} \right) = \frac{1}{2} \left((M_{11} + M_{22}) \pm \sqrt{(M_{11} - M_{22})^2 + 4|M_{12}|^2} \right). \quad (188)$$

Here both P and Q can be written as a sum of several whole square terms and thus they are both positive definite for any algebra elements a . Clearly,

$$E_+ \geq E_- \quad \forall a \in B \quad (189)$$

yielding, for a particular $a \in B$,

$$\|[\mathcal{D}, \pi(a)]\|_{op} = \frac{1}{r_1} \sqrt{E_+}. \quad (190)$$

The corresponding infimum $\inf_{a \in B} \|\mathcal{D}, \pi(a)\|_{\text{op}}$ is computed by varying the entries in the algebra elements, within the admissible ranges and obtaining the global minimum of E_+ . This gives

$$\inf_{a \in B} \|\mathcal{D}, \pi(a)\|_{\text{op}} = \frac{1}{r_1} \min(\sqrt{E_+}) = \frac{1}{r_1} \sqrt{\min(E_+)}. \quad (191)$$

The eigenvalue E_+ will always have a ‘‘concave-up’’ structure in the parametric space as it can be written as the sum of square terms only (187) and (188). There can be points in the parametric space where E_+ and E_- are equal, namely points where Q becomes 0, but since E_+ can not become less than E_- , determining the minimum of E_+ will alone suffice in calculating the infimum of the operator norm as is clear from (190). So we work with E_+ alone and use *Mathematica* to get the desired result.

The pure states corresponding to points on the fuzzy sphere can be obtained by the action of the $SU(2)$ group element

$$\hat{U} = e^{i\theta \hat{J}_2} = \begin{pmatrix} \cos^2 \frac{\theta}{2} & \frac{1}{\sqrt{2}} \sin \theta & \sin^2 \frac{\theta}{2} \\ -\frac{1}{\sqrt{2}} \sin \theta & \cos \theta & \frac{1}{\sqrt{2}} \sin \theta \\ \sin^2 \frac{\theta}{2} & -\frac{1}{\sqrt{2}} \sin \theta & \cos^2 \frac{\theta}{2} \end{pmatrix} \quad (192)$$

on the pure state $|1\rangle\langle 1|$ corresponding to the north pole (N) of \mathbb{S}_*^2 (with $n = 1$) i.e. $\rho_\theta = \hat{U}|1\rangle\langle 1|\hat{U}^\dagger$. Note that we have taken for convenience the azimuthal angle $\phi = 0$. This can be done without loss of generality.

Correspondingly,

$$\Delta\rho = \rho_\theta - \rho_0 = \hat{U}|1\rangle\langle 1|\hat{U}^\dagger - |1\rangle\langle 1| = \begin{pmatrix} \cos^4 \frac{\theta}{2} - 1 & -\frac{1}{\sqrt{2}} \sin \theta \cos^2 \frac{\theta}{2} & \sin^2 \frac{\theta}{2} \cos^2 \frac{\theta}{2} \\ -\frac{1}{\sqrt{2}} \sin \theta \cos^2 \frac{\theta}{2} & \frac{1}{2} \sin^2 \theta & -\frac{1}{\sqrt{2}} \sin \theta \sin^2 \frac{\theta}{2} \\ \sin^2 \frac{\theta}{2} \cos^2 \frac{\theta}{2} & -\frac{1}{\sqrt{2}} \sin \theta \sin^2 \frac{\theta}{2} & \sin^4 \frac{\theta}{2} \end{pmatrix} \quad (193)$$

like the $n = 1/2$ case (165), all entries are real here; indeed by writing $\Delta\rho = (\Delta\rho)_i \lambda_i$ (λ_i 's are the Gell-Mann matrices) the coefficients of λ_2 , λ_5 and λ_7 vanishes. This $\Delta\rho$ however only provides us with a lower bound (42) of the distance in Connes' formula and the actual distance is reached by some optimal algebra element (a_S) of the form

$$a_S = \Delta\rho + \kappa \Delta\rho_\perp ; \quad \text{tr}(\Delta\rho \Delta\rho_\perp) = 0, \quad (194)$$

for which the infimum is reached (say in (55)). This should be contrasted with the optimal element, for which the supremum is reached in (144). In any case, let us first try to have an improved estimate of the upper bound of the distance. This will be followed by the computation involving $\Delta\rho_\perp$.

6.7.2 An improved but realistic estimate of spectral distance

The upper bound for the spectral distance, obtained previously in (144) corresponded to that of a commutative sphere \mathbb{S}^2 , but that lies much above the realistic distance for any fuzzy sphere \mathbb{S}_*^2 associated to the n -representation of $SU(2)$, as discussed in section 6.2. It is therefore quite imperative that we try to have a more realistic estimate of this where this upper bound will be lowered considerably. At this stage, we can recall the simple example of H_2 -atom, where the energy gap between the ground state ($n = 1$) and first excited state ($n = 2$) is the largest one and the corresponding gaps in the successive energy levels go on decreasing and virtually become continuous for very large n ($n \gg 1$). One can therefore expect a similar situation here too. Indeed, a preliminary look into the distance between north and south poles (135) already support this in the sense that $\frac{(d_{3/2(N,S)}/r_{3/2})}{(d_{1(N,S)}/r_1)} < \frac{(d_{1(N,S)}/r_1)}{(d_{1/2(N,S)}/r_{1/2})}$. One therefore expects the distance function $d_1(\rho_0, \rho_\theta)$ to be essentially of the same form as that of $d_{1/2}(\rho_0, \rho_\theta)$, except to be scaled up by a $\sqrt{2}$ -factor and a miniscule deformation in the functional form. For large-values of n , the corresponding ratios $\frac{(d_n(N,S)/r_n)}{(d_{n-1(N,S)}/r_{n-1})} \rightarrow 1$, and the functional deformations are expected to be pronounced. However, the exact determination of this form is extremely difficult and we will have to be content with a somewhat heuristic analysis in this subsection and a more careful analysis, using (55), in the next subsection. To that end, we start here with the most general form of an algebra element a , as a linear combination of all the 8 Gell-Mann matrices (λ_i) and look for an optimal element from $a \in B$ giving $\sup |(\Delta\rho, a)|$, with some additional restrictions which are to be discussed later. We write

$$a = x_i \lambda_i = \begin{pmatrix} x_3 + \frac{x_8}{\sqrt{3}} & x_1 - ix_2 & x_4 - ix_5 \\ x_1 + ix_2 & -x_3 + \frac{x_8}{\sqrt{3}} & x_6 - ix_7 \\ x_4 + ix_5 & x_6 + ix_7 & -\frac{2x_8}{\sqrt{3}} \end{pmatrix} \quad (195)$$

in analogy with (157) for $n = 1/2$ \mathbb{S}_*^2 . Again the rows/columns are labeled from top to bottom/left to right by $(\langle 1|, \langle 0|, \langle -1|)/(|1\rangle, |0\rangle, |-1\rangle)$. Now we calculate $\text{tr}(\Delta\rho a)$ using the $\Delta\rho$ matrix (193) and the above algebra element (195) to get

$$\text{tr}(\Delta\rho a) = \left(x_3 + \frac{x_8}{\sqrt{3}}\right) \left(\cos^4 \frac{\theta}{2} - 1\right) - \frac{2x_8}{\sqrt{3}} \sin^4 \frac{\theta}{2} + \frac{x_4}{2} \sin^2 \theta + \frac{1}{2} \sin^2 \theta \left(\frac{x_8}{\sqrt{3}} - x_3\right) - \sqrt{2} \sin \theta \left(x_1 \cos^2 \frac{\theta}{2} + x_6 \sin^2 \frac{\theta}{2}\right). \quad (196)$$

This clearly demonstrates the expected independence of imaginary components viz. x_2, x_5 and x_7 . We therefore set $x_2 = x_5 = x_7 = 0$ to begin with. This simplifies the matrix elements of M (187), using (195), as

$$M_{11} = 3x_1^2 + 6x_4^2 + 8x_3^2 + (x_6 - 2x_1)^2, \quad (197)$$

$$M_{22} = 3x_6^2 + 6x_4^2 + (x_1 - 2x_6)^2 + 2\left(\sqrt{3}x_8 - x_3\right)^2, \quad (198)$$

$$M_{12} = \sqrt{2}\left(3x_4(x_1 + x_6) + 2x_3(x_1 - 2x_6) - (2x_1 - x_6)(x_3 - \sqrt{3}x_8)\right). \quad (199)$$

Like-wise the above expression (196) simplifies as

$$|tr(\Delta\rho a)| = \left| \left[\sin\left(\frac{\theta}{2}\right) \left\{ \sin\left(\frac{\theta}{2}\right) \left\{ x_3 + 3x_3 \cos^2\left(\frac{\theta}{2}\right) + \sqrt{3}x_8 \sin^2\left(\frac{\theta}{2}\right) \right\} \right. \right. \right. \\ \left. \left. \left. + \cos\left(\frac{\theta}{2}\right) \left\{ 2\sqrt{2}x_1 \cos^2\left(\frac{\theta}{2}\right) + 2\sqrt{2}x_6 \sin^2\left(\frac{\theta}{2}\right) - 2x_4 \sin\left(\frac{\theta}{2}\right) \cos\left(\frac{\theta}{2}\right) \right\} \right\} \right] \right|. \quad (200)$$

Our aim is to obtain a simple form of the ‘‘Ball’’ condition and eventually of Connes spectral distance (33) so that we might obtain an improved estimate for the spectral distance over the lower bound (42), obtained by making use of $\Delta\rho$ (193), which is more realistic than (144). We shall see shortly that with few more additional restrictions, apart from the previous ones (like vanishing of x_2, x_5 and x_7 imposed already) it is possible to simplify the analysis to a great extent, which in turn yields a distance estimate which has the same mathematical structure as that of the exact distance (167) for the $n = 1/2$ case upto an overall factor. To that end, we impose the following new constraints:

$$x_1 = x_6; \quad x_3 = \frac{x_8}{\sqrt{3}}; \quad x_4 = 0, \quad (201)$$

as a simple observation of (200) suggests that it simplifies even further to the following form:

$$|tr(\Delta\rho a)| = \left| \left[\sin\left(\frac{\theta}{2}\right) \left\{ 4x_3 \sin\left(\frac{\theta}{2}\right) + 2\sqrt{2}x_1 \cos\left(\frac{\theta}{2}\right) \right\} \right] \right| = 2\sqrt{2}\sqrt{x_1^2 + 2x_3^2} \left| \sin\left(\frac{\theta}{2}\right) \cos\left(\zeta - \frac{\theta}{2}\right) \right|, \quad (202)$$

where $\cos\zeta = \frac{x_1}{\sqrt{x_1^2 + 2x_3^2}}$ and $\sin\zeta = \frac{\sqrt{2}x_3}{\sqrt{x_1^2 + 2x_3^2}}$. Moreover, putting the above constraints (201) in the equation (197)-(199), we get

$$M_{11} = M_{22} = 4x_1^2 + 8x_3^2; \quad M_{12} = 0. \quad (203)$$

With this, the eigenvalue E_+ (188) and the corresponding ball condition (190) can be obtained as

$$E_+ = 4x_1^2 + 8x_3^2 \Rightarrow \|[D, \pi(a)]\|_{\text{op}} = \frac{1}{r_1} 2\sqrt{x_1^2 + 2x_3^2} \leq 1. \quad (204)$$

Using this ball condition in (202), we get

$$|tr(\Delta\rho a)| \leq \sqrt{2}r_1 \sin\left(\frac{\theta}{2}\right) \cos\left(\zeta - \frac{\theta}{2}\right). \quad (205)$$

Hence, a suggestive form of the spectral distance between a pair of pure states $\rho_0 = |1\rangle\langle 1|$ and $\rho_\theta = U|1\rangle\langle 1|U^\dagger$ for the $n = 1$ representation can be easily obtained by identifying the optimal value of the last free parameter ζ to be given by $\zeta = \frac{\theta}{2}$. This yields

$$d_1^a = \sup_{a \in B} \{|tr(\Delta\rho a)|\} = \sqrt{2}r_1 \sin\left(\frac{\theta}{2}\right). \quad (206)$$

The corresponding form of the optimal algebra element a_s is obtained after a straightforward computation to get

$$\hat{a}_s = \frac{r_1}{2} \begin{pmatrix} \sqrt{2} \sin\left(\frac{\theta}{2}\right) & \cos\left(\frac{\theta}{2}\right) & 0 \\ \cos\left(\frac{\theta}{2}\right) & 0 & \cos\left(\frac{\theta}{2}\right) \\ 0 & \cos\left(\frac{\theta}{2}\right) & -\sqrt{2} \sin\left(\frac{\theta}{2}\right) \end{pmatrix}. \quad (207)$$

When $\theta = \pi$, the distance is exactly the same between the two pure coherent states $|1\rangle\langle 1|$ and $|-1\rangle\langle -1|$ and the above distance (206) gives $d_1^a(\rho_0, \rho_\pi) = \sqrt{2}r_1$ which exactly matches with the one computed in (135) using the discrete formula (134).

Note that we have made use of all the restrictions $x_2 = x_4 = x_5 = x_1 - x_6 = x_3 - \frac{x_8}{\sqrt{3}} = 0$ and $\zeta = \frac{\theta}{2}$, imposed at various stages. Finally, we would like to mention that this simple form (206) was obtained by imposing the above ad-hoc constraints resulting in $M_{11} - M_{22} = M_{12} = 0$. Consequently, one cannot a priori expect this to reflect the realistic distance either. At best, this can be expected to be closer to the realistic one, compared to (144). The only merit in (206) is that it has essentially the same structure as that of (167) for the $n = \frac{1}{2}$ case. Nevertheless, as we shall show below, the computation involving $\Delta\rho_\perp$, using (54)-(55) matches with (206) to a great degree of accuracy.

Note that we are denoting the analytical distances as (d^a) to distinguish them from other distances to be calculated in the next section. Also note that since the analytical distance (206) has the same form as (167), it corresponds to

$\sqrt{2}$ -times the half of the chordal distance. Furthermore, it satisfies the Pythagoras equality (176) just like the $n = \frac{1}{2}$ case.

Before we conclude this subsection, we would like to point out that we could have perhaps reversed our derivation by simply requiring the matrix M (187) to be diagonal: $M_{12} = 0$. But in that case $E_+ = \max\{M_{11}(a), M_{22}(a)\}$ for a particular choice of algebra element, satisfying the aforementioned conditions viz $x_2 = x_5 = x_7 = M_{12} = 0$. Now given the structures of M_{11} (197) and M_{22} (198) they will have shapes which are concave upwards, when the hyper-surfaces are plotted against the set of independent parameters occurring in 'a' $\in \mathcal{R}$, where \mathcal{R} represents the subregion in the parameter space, defined by these conditions. Now it may happen that $M_{11}(a) \neq M_{22}(a)$, $\forall a \in \mathcal{R}$, in which case one of them, say $M_{11}(a)$, exceeds the other: $M_{11} > M_{22}$. Then clearly

$$\inf_{a \in \mathcal{R}} \|\mathcal{D}, \pi(a)\|_{\text{op}} = \frac{1}{r_1} \sqrt{\min_{a \in \mathcal{R}}(M_{11})}. \quad (208)$$

Otherwise, the hyper-surfaces given by $M_{11}(a)$ and $M_{22}(a)$ will definitely intersect and (208) will reduce to

$$\inf_{a \in \bar{\mathcal{R}}} \|\mathcal{D}, \pi(a)\|_{\text{op}} = \frac{1}{r_1} \sqrt{\min_{a \in \bar{\mathcal{R}}}(M_{11})} = \frac{1}{r_1} \sqrt{\min_{a \in \bar{\mathcal{R}}}(M_{22})}, \quad (209)$$

where $\bar{\mathcal{R}} \subset \mathcal{R}$ represents the subregion where $M_{11}(a) = M_{22}(a)$. In fact, this is a scenario which is more likely in this context, as suggested by our analysis of infinitesimal distance presented in the next subsection (see also Fig. 2). We therefore also set $M_{11} = M_{22}$. With the additional condition like $x_1 = x_6$ (201), we can easily see that one gets, apart from (201), another set of solutions like,

$$x_1 = x_6, \quad x_3 = -\sqrt{3}x_8, \quad x_4 = -\frac{2}{\sqrt{3}}x_8. \quad (210)$$

This, however, yields the following ball condition

$$\sqrt{x_1^2 + 8x_8^2} \leq \frac{r_1}{2}, \quad (211)$$

the counterpart of (204), and in contrast to (202), cannot in anyway be related to its counterpart here, given by

$$|\text{tr}(\Delta\rho a)| = \sqrt{\frac{2}{3}} \sin\theta (\sqrt{2}x_8 \sin\theta - \sqrt{3}x_1). \quad (212)$$

We therefore reject (210) from our consideration, as it will not serve our purpose.

6.7.3 Spectral distance using $\Delta\rho_{\perp}$

In this section we employ the modified distance formula (54) by constructing the most general form of $\Delta\rho_{\perp}$ for both finite as well as infinitesimal distances. We show that in both of the cases the distance calculated using this more general (numerical) method matches with the corresponding result given by d^a (206) to a very high degree of accuracy suggesting that d^a should be the almost correct distance for arbitrary θ .

6.7.3.1 Infinitesimal distance

In this case $d\rho$ takes a simpler form by expanding (193) and keeping only the leading order terms in $d\theta$:

$$d\rho = \rho_{d\theta} - \rho_0 = -\frac{d\theta}{\sqrt{2}} (|1\rangle\langle 0| + |0\rangle\langle 1|). \quad (213)$$

The most general structure of the transverse part $d\rho_{\perp}$ here is obtained by taking all possible linear combinations of the generic states $|i\rangle\langle j|$ i.e.

$$d\rho_{\perp} = \sum_{i,j} C_{ij} |i\rangle\langle j| \quad ; \quad i, j \in \{-1, 0, +1\}, \quad (214)$$

where $C_{ij} = C_{ji}^*$ because of the hermiticity of $d\rho_{\perp}$. Clearly, the complex parameters C_{ij} are exact analogues of suitable combinations of x_i 's in (195). The orthogonality condition (194) here requires the coefficient C_{10} to be purely imaginary. Moreover we can demand that the matrix representation of $\Delta\rho_{\perp}$ should be traceless as discussed in section 6.7. We thus impose $C_{11} + C_{22} + C_{33} = 0$. To better understand the significance of each term we write (214) in matrix form as follows:

$$d\rho_{\perp} = \begin{pmatrix} \mu_1 & i\alpha_1 & \gamma \\ -i\alpha_1 & \mu_0 & \beta \\ \gamma^* & \beta^* & -(\mu_1 + \mu_0) \end{pmatrix} ; \quad \mu_1, \mu_0, \mu_{-1}, \alpha_1 \in \mathbb{R} \quad \text{and} \quad \beta, \gamma \in \mathbb{C}. \quad (215)$$

With this our optimal algebra element a_S (194) becomes:

$$a_S = \begin{pmatrix} \mu_1 & -\frac{d\theta}{\sqrt{2}} + i\alpha_1 & \gamma \\ -\frac{d\theta}{\sqrt{2}} - i\alpha_1 & \mu_0 & \beta \\ \gamma^* & \beta^* & -(\mu_1 + \mu_0) \end{pmatrix}, \quad (216)$$

where we have absorbed κ inside the coefficients of $d\rho_{\perp}$ (215). With 7 independent parameters, it is extremely difficult to vary all the parameters simultaneously to compute the infimum analytically. However, as far as infinitesimal distances are concerned, it may be quite adequate to take each parameter to be non-vanishing one at a time. Thus, by keeping one of these diagonal/complex conjugate pairs like β and γ to be non-zero one at a time and computing the eigenvalues of the 2×2 matrix (187) using (194), (213) and (215), it is found that only the real part of β contributes non-trivially to the infimum of the operator norm $\|[\mathcal{D}, \pi(a)]\|_{\text{op}}$ in the sense that the operator norm of this object

with $a_S = \begin{pmatrix} 0 & -\frac{d\theta}{\sqrt{2}} & 0 \\ -\frac{d\theta}{\sqrt{2}} & 0 & \beta \\ 0 & \beta^* & 0 \end{pmatrix}$ in (194) is a monotonically increasing function of $Im(\beta)$ but yields a non-trivial value

for the infimum which is less than the one with vanishing β i.e. $d\rho$ itself. Like-wise, both real and imaginary parts of γ and α_1 in (215) does not contribute to the infimum.

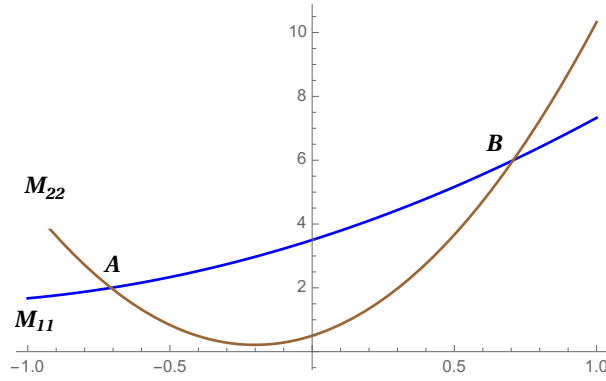


Figure 2: Infimum corresponding to the plots of M_{11} and M_{22}

On computation, we get

$$\|[\mathcal{D}, \pi(a)]\|_{\text{op}} = \frac{1}{r_1} \sqrt{\max\{M_{11}, M_{22}\}}, \quad \text{where } M_{11} = \beta_1^2 + 2\sqrt{2}\beta_1 d\theta + \frac{7}{2}d\theta^2 \quad \text{and} \quad M_{22} = 7\beta_1^2 + 2\sqrt{2}\beta_1 d\theta + \frac{1}{2}d\theta^2; \quad (217)$$

where $\beta_1 = Re(\beta)$ and the 2×2 matrix (187) takes a diagonal form $diag\{M_{11}, M_{22}\}$ thus trivially yielding eigenvalues (217). From the plot of these eigenvalues (see Fig.2) it is clear that the infimum of the operator norm over the full range of β_1 is given by the minimum value of the two intersections at A ($\beta_1 = -\frac{d\theta}{\sqrt{2}}$) and B ($\beta_1 = +\frac{d\theta}{\sqrt{2}}$) which comes out to be $\frac{\sqrt{2}d\theta}{r_1}$ i.e. $\|[\mathcal{D}, \pi(a)]\|_{\text{op}} = \frac{\sqrt{2}d\theta}{r_1}$. Note in this context that

$$E_+ = \begin{cases} M_{22}, & \text{for } \beta_1 < -\frac{d\theta}{\sqrt{2}} \quad \text{and} \quad \beta_1 > +\frac{d\theta}{\sqrt{2}} \quad \text{i.e. left of A and right of B} \\ M_{11}, & \text{for } -\frac{d\theta}{\sqrt{2}} < \beta_1 < +\frac{d\theta}{\sqrt{2}} \quad \text{i.e. in between A and B.} \end{cases}$$

Also, since $\|d\rho\|_{tr}^2 = d\theta^2$, as follows from (213), the infinitesimal spectral distance (54) is given by

$$d_1(\rho_{d\theta}, \rho_0) = r_1 \frac{d\theta}{\sqrt{2}}. \quad (218)$$

We now corroborate the same result by varying all the 7 parameters simultaneously. Of course we shall have to employ *Mathematica* now. To that end, first note that P, Q (187) and (188) are now given as:

$$P = 2\{1 + \mu_1^2 + 2\beta_1^2 + 3\alpha^2 + 4\mu_0^2 + 6|\gamma|^2 + (\mu_1 + \mu_0)^2 + (\sqrt{2}\beta_1 + 1)^2 + (2\beta_2 - \alpha)^2\}, \quad (219)$$

$$Q = 9\{-1 + 4\mu_0\mu_1 + 2(|\beta|^2 + \mu_0^2 - \alpha^2)\}^2 + 4\{3(\mu_0 + \mu_1 + \gamma_1) + 4.242(\beta_1\mu_1 - \beta_2\gamma_2 - \alpha\gamma_2 - \beta_1\gamma_1)\}^2 + 4\{3\gamma_2 + 4.242(\beta_2\mu_1 + \beta_2\gamma_1 + \alpha\gamma_1 - \beta_1\gamma_2 - \alpha\mu_0 - \alpha\mu_1)\}^2, \quad (220)$$

where $\beta = \beta_1 + i\beta_2$ and $\gamma = \gamma_1 + i\gamma_2$. Interestingly enough we get the same infimum i.e. $2d\theta^2$ by finding the minimum of the eigenvalue E_+ as discussed in section 6.7.1 with the 7 parameter eigenvalue (188) where P and Q are given by (219) and (220). We therefore recover the distance (218) which also matches with (206) for $\theta \rightarrow d\theta$.

6.7.3.2 Finite distance

For any finite angle θ , the $\Delta\rho$ matrix (193) can be directly used to compute the square of the trace norm $\|\Delta\rho\|_{tr}^2$. Moreover, this $\Delta\rho$ can be used as the algebra element a to compute the eigenvalues of (188) and then the operator

norm $\|\mathcal{D}, \pi(a)\|_{op}$, yielding the lower bound for the spectral distance using (42). More specifically for $\theta = \frac{\pi}{2}$ (i.e. the distance between the north pole N and any point E on the equator) the lower bound is found to be

$$d_1(N, E) \geq 0.699r_1. \quad (221)$$

Contrasting with the corresponding value (206) of $d_1^a = \sqrt{2}r_1 \sin(\frac{\pi}{4}) = r_1$, we see that the transverse component $\Delta\rho_\perp$ must play a role here. On the other hand for $\theta = \pi$ (i.e. the distance between north and south pole) we find $d(N, S) = \sqrt{2}r_1$ which matches exactly with the result of (135) for the distance between discrete states $|1\rangle\langle 1|$ and $|-1\rangle\langle -1|$. This means that there is no contribution of $\Delta\rho_\perp$ to this distance for $\theta = \pi$. There are, however, non-trivial contributions from $\Delta\rho_\perp$ to the distance for any general value of the angle $\theta < \pi$ as we have illustrated above through the example of $\theta = \frac{\pi}{2}$. Now the most general $\Delta\rho_\perp$ in this case can be constructed as follows:

$$\begin{aligned} \Delta\rho_\perp = & [\mu_1|1\rangle\langle 1| + \mu_0|0\rangle\langle 0| + \mu_{-1}|-1\rangle\langle -1| + \alpha|1\rangle\langle 0| + \alpha^*|0\rangle\langle 1| \\ & + \gamma|1\rangle\langle -1| + \gamma^*|-1\rangle\langle 1| + \beta|0\rangle\langle -1| + \beta^*|-1\rangle\langle 0|], \end{aligned} \quad (222)$$

where $\mu_1, \mu_0, \mu_{-1} \in \mathbb{R}$. Again we can take a_S (194) to be traceless as before, which implies $\mu_1 + \mu_0 + \mu_{-1} = 0$ and we can eliminate one of them, say μ_{-1} . Furthermore, imposing the orthogonality condition (194) we have a relation between all the remaining 8 parameters and one of them can be eliminated from that. In this case, using the $\Delta\rho$ (193) and $\Delta\rho_\perp$ (222) in (194) while absorbing κ inside the coefficients of $\Delta\rho_\perp$, we have

$$\text{tr}(\Delta\rho \Delta\rho_\perp) = 0 \implies \mu_1 = -\frac{1}{2}\mu_0 \sin^2\left(\frac{\theta}{2}\right) - \frac{1}{\sqrt{2}}\beta_1 \sin\theta + \cos^2\left(\frac{\theta}{2}\right) \left(\gamma_1 + \mu_0 - \sqrt{2}\alpha_1 \cot\frac{\theta}{2}\right), \quad (223)$$

where α_1, β_1 and γ_1 are the real components and α_2, β_2 and γ_2 are the imaginary components of α, β and γ respectively. With these substitutions the eigenvalues of the matrix (187) become a function of 7 parameters. We now calculate P,Q (188) for the $\theta = \frac{\pi}{2}$ case to get

$$\begin{aligned} P = & 5 + \frac{45}{4}\mu_0^2 + 8(|\alpha|^2 + |\beta|^2) + 2(\alpha_1^2 + \beta_1^2) + \gamma_1^2 + 12|\gamma|^2 - 4\gamma_1 + 6\mu_0 \\ & - 3\sqrt{2}\mu_0(\beta_1 + \alpha_1) - 4\alpha_1\beta_1 + 3\gamma_1\mu_0 - 2\sqrt{2}\gamma_1(\beta_1 + \alpha_1) - 8\alpha_2\beta_2, \end{aligned} \quad (224)$$

$$\begin{aligned} Q = & 9\left[1 + 2|\alpha|^2 - 3\mu_0^2 - 2|\beta|^2 - \gamma_1 + \frac{1}{2}\mu_0 + 2\sqrt{2}\beta_1 - 2\mu_0\gamma_1 + 2\sqrt{2}\mu_0(\alpha_1 + \beta_1)\right]^2 + \frac{1}{2}\left\{(\sqrt{2} + 2\sqrt{2}\alpha_1^2 - 2\sqrt{2}\beta_1^2 \right. \\ & + 2\sqrt{2}\gamma_1 - 4\beta_1 + \sqrt{2}\mu_0 + \mu_0\beta_1 - 4\gamma_2\beta_2 - 6\gamma_1\alpha_1 - 4\gamma_2\alpha_2 - 5\alpha_1\mu_0)^2 + (2\beta_2 - 2\sqrt{2}\gamma_2 - 2\alpha_2 - 6\gamma_1\beta_2 \\ & \left. - 2\sqrt{2}\alpha_1\alpha_2 + 4\alpha_1\gamma_2 + 2\sqrt{2}\alpha_1\beta_2 + \beta_2\mu_0 + 4\gamma_2\beta_1 + 2\sqrt{2}\beta_1\beta_2 - 2\gamma_1\alpha_2 + 5\alpha_2\mu_0 - 2\sqrt{2}\beta_1\alpha_2)^2\right\}. \end{aligned} \quad (225)$$

Minimizing E_+ as before, we get

$$d(N, E) = r_1, \quad (226)$$

which, remarkably, exactly matches the result of (206). As for $\theta = \pi$, the terms P,Q (188) of the eigenvalues E_\pm come out to be

$$P = 4 + 9\mu_0^2 + 8(|\alpha|^2 + |\beta|^2) + 12|\gamma|^2 - 8(\alpha_1\beta_1 + \alpha_2\beta_2), \quad (227)$$

$$\begin{aligned} Q = & 36(|\beta|^2 - |\alpha|^2 - 2\mu_0)^2 + 18\left[\left\{(\beta_1 + \alpha_1)(2\gamma_1 + \mu_0) + 2(\beta_1 - \alpha_1) + 2\gamma_2(\alpha_2 + \beta_2)\right\}^2 \right. \\ & \left. + \left\{(\beta_2 + \alpha_2)(2\gamma_1 - \mu_0) - 2(\beta_2 - \alpha_2) - 2\gamma_2(\alpha_1 + \beta_1)\right\}^2\right]. \end{aligned} \quad (228)$$

Again we need to calculate the spectral distance by minimizing E_+ which gives $d_1(\rho_{\theta=\pi}, \rho_0) = \sqrt{2}r_1$. This is precisely the lower bound result $d_1(N, S)$ of (135) as discussed previously and hence support our claim that $\Delta\rho_\perp$ will not contribute here at all. For arbitrary angle θ , we present in Table 1 both the distances i.e. the one calculated using the formula (206) and the other calculated using the global minima of the eigenvalue E_+ (say d_1) for various angles between 0 and π .

Angle (degree)	d_1^a/r_1	d_1/r_1
10	0.1232568334	0.1232518539
20	0.2455756079	0.2455736891
30	0.3660254038	0.3660254011
40	0.4836895253	0.4836894308
50	0.5976724775	0.5976724773
60	0.7071067812	0.7071067811
70	0.8111595753	0.8111595752
80	0.9090389553	0.9090389553
90	1	0.999999998
100	1.0833504408	1.0833504407
110	1.1584559307	1.1584559306
120	1.2247448714	1.2247448713
130	1.2817127641	1.2817127640
140	1.3289260488	1.3289260487
150	1.3660254038	1.3660254037
160	1.3927284806	1.3927284806
170	1.4088320528	1.4088320527

Table 1: Data set for various distances corresponding to different angles

It is very striking that the distance d_1^a (206) matches almost exactly with d_1 for all these angles as one sees from table 1. This strongly suggests that (206) is indeed very very close to the exact distance! In fact, for larger angles like 50° and above the results agree upto 9 decimal places, whereas for smaller angles ($< 50^\circ$) they agree upto 5 decimal places and show some miniscule deviations from 6 decimals onwards. One can expect to see more pronounced deformations away from (206) in the functional form when the overall scale of magnification starts reducing monotonically with $n \rightarrow \infty$ and eventually merge with the commutative results.

7 Conclusions

We have provided here a general algorithm to compute the finite spectral distance on non-commutative spaces, in our Hilbert-Schmidt operator formulation, and we find here that the formula quoted in [1] actually corresponds to the lower bound. However, as far as the computation of infinitesimal distances is concerned, this formula is quite adequate. This is because it can reproduce the local infinitesimal distance up to an overall numerical factor as shown in [1, 4]. We should, however, keep in mind that the knowledge of infinitesimal distances may not be adequate to capture the geometry of a generic non-commutative space as such spaces, unlike a commutative differentiable manifold, may not allow a geodesic to be defined in the conventional sense. By the word ‘‘conventional’’, we mean that the geodesic passes through a one parameter family of pure states. In this situation, one cannot simply integrate the infinitesimal distance to compute the finite distance.

Here, we have studied extensively the geometry of the Moyal plane (\mathbb{R}_*^2) and that of the Fuzzy sphere (\mathbb{S}_*^2). For this, we made use of both the above mentioned revised algorithm and also emulated the method of [2] to compute the upper bound and then look for an optimal element saturating this upper bound. In the case of the Moyal plane, we succeed in identifying such optimal element ‘ a_s ’ belonging to the multiplier algebra. We then constructed a sequence of projection operators $\pi^N(a_s)$ in the finite dimensional subspace spanned by eigen-spinors of the Dirac operator that converge to $\pi(a_s)$ and saturates the upper bound, allowing us to identify the upper bound itself with the distance. Eventually, this enables us to relate the one parameter family of pure states to the geodesic of the Moyal plane which is nothing but the straight line. In contrast, on the fuzzy sphere, although an analogous upper bound can be constructed for any finite n -representation of $su(2)$, there simply does not exist an optimal element a_s saturating the inequality. Indeed, for the case of extremal non-commutativity $n = \frac{1}{2}$, the finite distance turns out to be half the chordal distance. Here, except for the extremal points, the interpolating ‘‘points’’ correspond to mixed states. This in turn helps us to find the distance between a given mixed state and a uniquely defined nearest pure state lying on the ‘‘surface’’ of \mathbb{S}_*^2 . The corresponding distance can then be taken as an alternative characterization of the ‘‘mixedness’’ of a state. This exercise shows that in Connes’ framework no discrimination is made between pure and mixed states; it scans through the entire set of pure and mixed states to compute the supremum in (33).

All these calculations are enormously simplified by working in the eigen-spinor basis of the respective Dirac operator, so much so that we are able to compute the distance in the ‘ $n = 1$ ’ fuzzy sphere, using this revised algorithm. Since this algorithm involves also the transverse $\Delta\rho_\perp$ components in addition to the longitudinal $\Delta\rho$ component, this becomes somewhat less user-friendly. For the ‘ $n = 1$ ’ case, for example, it involves a minimization in seven parameters. Needless to say that we have to make use of *Mathematica* after solving the quadratic characteristic equation. For higher n ’s, the corresponding characteristic equations will not only involve higher degree polynomials, it will also involve a large number of independent parameters to be varied. Consequently, the computation for the $n > 1$ fuzzy sphere, even with the help of *Mathematica*, remains virtually intractable and for the Moyal plane the number of parameters is simply infinite! To put our findings in a nutshell, we observe that the finite distance for

$n = 1$ and that of $n = \frac{1}{2}$ have almost the same functional form except for an overall scaling by a factor of $\sqrt{2}$ and a miniscule deformation at small ‘ θ ’ and that too only from the sixth decimal onwards.

8 Acknowledgements

We thank Prof. A.P. Balachandran for his valuable suggestions. AP thanks the INSPIRE and KK thanks SNBNCBS for the financial support to carry out their project works. Both of them thank SNBNCBS for the hospitality during their stay when parts of this work were completed.

Appendix

A.1 Dirac Operator in Moyal plane, its response to $ISO(2)$ symmetry and a useful identity

In order to construct a Dirac Operator for the Moyal plane, we need to consider the momentum operator satisfying the non-commutative Heisenberg algebra (1, 3). Now since only \mathcal{H}_q can furnish a complete representation of the entire Heisenberg algebra we need to construct our Dirac operator on this space. Thus we consider the operators \hat{P}_α , which acts adjointly only on \mathcal{H}_q . The Dirac operator is then constructed in terms of Pauli matrices $\sigma_1 = \begin{pmatrix} 0 & 1 \\ 1 & 0 \end{pmatrix}$ and

$$\sigma_2 = \begin{pmatrix} 0 & -i \\ i & 0 \end{pmatrix} \text{ as}$$

$$\mathcal{D} \equiv \sigma_i \hat{P}_i = \sigma_1 \hat{P}_1 + \sigma_2 \hat{P}_2. \quad (229)$$

Note that in this construction the Dirac operator has a natural action on $\mathcal{H}_q \otimes \mathbb{C}^2$ through the adjoint action of \hat{P}_i , i.e. on a generic element $\Phi = \begin{pmatrix} |\phi_1\rangle \\ |\phi_2\rangle \end{pmatrix} \in \mathcal{H}_q \otimes \mathbb{C}^2$ it acts as

$$\mathcal{D}\Phi = \sqrt{\frac{2}{\theta}} \begin{pmatrix} [i\hat{b}^\dagger, |\phi_2\rangle] \\ [-i\hat{b}, |\phi_1\rangle] \end{pmatrix}. \quad (230)$$

This, on turn implies that the action of the commutator $[\mathcal{D}, \pi(a)]$ on Φ , on using (25), gives

$$[\mathcal{D}, \pi(a)]\Phi = \sqrt{\frac{2}{\theta}} \begin{pmatrix} 0 & [i\hat{b}^\dagger, a] \\ [-i\hat{b}, a] & 0 \end{pmatrix} \Phi. \quad (231)$$

Now regarding Φ as a test function, we can identify the Dirac operator \mathcal{D} as

$$\mathcal{D} = \sqrt{\frac{2}{\theta}} \begin{pmatrix} 0 & i\hat{b}^\dagger \\ -i\hat{b} & 0 \end{pmatrix}. \quad (232)$$

This is further simplified by considering the transformation $\hat{b} \rightarrow i\hat{b}$ and $\hat{b}^\dagger \rightarrow -i\hat{b}^\dagger$, which just corresponds to a $SO(2)$ rotation by an angle $\pi/2$ in \hat{x}_1, \hat{x}_2 space. With this transformation the Dirac operator takes the following hermitian form :

$$\mathcal{D} = \sqrt{\frac{2}{\theta}} \begin{pmatrix} 0 & \hat{b}^\dagger \\ \hat{b} & 0 \end{pmatrix}, \quad (233)$$

which precisely has the same form as (26), used throughout the paper. The most important point to note is that this very structure of the Dirac operator allows us to make it also act directly from the left on $\Psi = \begin{pmatrix} |\psi_1\rangle \\ |\psi_2\rangle \end{pmatrix} \in \mathcal{H}_c \otimes \mathbb{C}^2$ (27). In this context, we would like to mention that this Dirac operator \mathcal{D} responds to a $SO(2)$ rotation in the \hat{x}_1, \hat{x}_2 plane by an arbitrary angle α as

$$\mathcal{D} = \sqrt{\frac{2}{\theta}} \begin{pmatrix} 0 & \hat{b}^\dagger \\ \hat{b} & 0 \end{pmatrix} \longrightarrow \mathcal{D}^{(\alpha)} = \sqrt{\frac{2}{\theta}} \begin{pmatrix} 0 & \hat{b}^{(\alpha)\dagger} \\ \hat{b}^{(\alpha)} & 0 \end{pmatrix} = \sqrt{\frac{2}{\theta}} \begin{pmatrix} 0 & \hat{b}^\dagger e^{-i\alpha} \\ \hat{b} e^{i\alpha} & 0 \end{pmatrix}. \quad (234)$$

Since $[\hat{b}^{(\alpha)}, \hat{b}^{(\alpha)\dagger}] = [\hat{b}, \hat{b}^\dagger] = 1$, one can build the tower of states, parametrized by α , analogous to (4) and is related to the ones in (4) by a phase factor:

$$|n\rangle^{(\alpha)} = \frac{(\hat{b}^{(\alpha)\dagger})^n}{\sqrt{n!}} |0\rangle = e^{-in\alpha} |n\rangle. \quad (235)$$

On the other hand, under translation (8), the Dirac operator transforms as

$$\mathcal{D} \rightarrow \mathcal{D}^{(z)} = U(z, \bar{z}) \mathcal{D} U^\dagger(z, \bar{z}) = \sqrt{\frac{2}{\theta}} \begin{pmatrix} 0 & \hat{b}^\dagger - \bar{z} \\ \hat{b} - z & 0 \end{pmatrix}. \quad (236)$$

Since the operators \hat{b} and \hat{b}^\dagger are shifted by a c-numbers only, it has no impact on the commutator $[\mathcal{D}, \pi(a)]$ occurring in the ball condition (33). Finally, note that the Dirac operator here is hermitian and differs from that of [1] by a factor $(-i)$, which however, is quite inconsequential as it does not affect the operator norm $\|[\mathcal{D}, \pi(a)]\|_{\text{op}}$, that appears in the ball condition (33).

We are now going to prove an identity that will be used in our calculations throughout the paper. For our Dirac operator (233) we have for $a \in \mathcal{A} = \mathcal{H}_q$

$$[\mathcal{D}, \pi(a)] = \sqrt{\frac{2}{\theta}} \begin{pmatrix} 0 & [\hat{b}, \pi(a)] \\ [\hat{b}^\dagger, \pi(a)] & 0 \end{pmatrix}, \quad (237)$$

yielding

$$\|[\mathcal{D}, \pi(a)]^\dagger [\mathcal{D}, \pi(a)]\|_{\text{op}} = \frac{2}{\theta} \text{Max} \left(\|\hat{Q}^\dagger \hat{Q}\|_{\text{op}}, \|\hat{Q} \hat{Q}^\dagger\|_{\text{op}} \right), \quad (238)$$

where we have introduced the operator \hat{Q} as

$$\hat{Q} = [\hat{b}^\dagger, \pi(a)] = -[\hat{b}, \pi(a)]^\dagger; \quad \hat{Q}^\dagger = [\hat{b}, \pi(a)]^\dagger = -[\hat{b}^\dagger, \pi(a)]. \quad (239)$$

Note that here the algebra element $a \in \mathcal{A} = \mathcal{H}_q$ has been taken to be hermitian ($a = a^\dagger$) since, as shown in [22], the optimal element for which the supremum in the Connes' distance formula is reached belongs to the subset of hermitian elements of the algebra \mathcal{A} .

We now state a theorem in standard functional analysis [23]:

Theorem :

If $A \in \mathcal{B}(\mathcal{H})$, we have $\|A\|_{\text{op}}^2 = \|A^*\|_{\text{op}}^2 = \|A^*A\|_{\text{op}}$, where the superscript $*$ stands for the involution operator.

From this theorem it then immediately follows that $\|\hat{Q}^\dagger \hat{Q}\|_{\text{op}} = \|\hat{Q} \hat{Q}^\dagger\|_{\text{op}}$. Since in our case the involution operation is given by the hermitian conjugation (\dagger), as mentioned earlier. Besides for a legitimate spectral triple $[\hat{b}, \pi(a)]$ and $[\hat{b}^\dagger, \pi(a)]$ both are bounded operators and thus the theorem holds.

We combine this result with (238) to obtain,

$$\|[\mathcal{D}, \pi(a)]\|_{\text{op}} = \sqrt{\frac{2}{\theta}} \|[\hat{b}^\dagger, \pi(a)]\|_{\text{op}} = \sqrt{\frac{2}{\theta}} \|[\hat{b}, \pi(a)]\|_{\text{op}}. \quad (240)$$

This simplifies the problem of finding the operator norm $\|[\mathcal{D}, \pi(a)]\|_{\text{op}}$ for any hermitian element $a \in \mathcal{A}$.

A.2 Fuzzy Sphere

A similar kind of identity also follows for the case of the fuzzy sphere. The Dirac operator for the fuzzy sphere is (30)

$$\mathcal{D} \equiv \frac{1}{r_n} \hat{J} \otimes \vec{\sigma} = \frac{1}{r_n} \begin{pmatrix} \hat{J}_3 & \hat{J}_- \\ \hat{J}_+ & -\hat{J}_3 \end{pmatrix}.$$

Then for a hermitian algebra element $a = a^\dagger \in \mathcal{A}$,

$$\begin{aligned} \|[\mathcal{D}, \pi(a)]\|_{\text{op}}^2 &= \|[\mathcal{D}, \pi(a)]^\dagger [\mathcal{D}, \pi(a)]\|_{\text{op}} \\ &= \frac{1}{r^2} \left\| \begin{bmatrix} [J_+, a]^\dagger [J_+, a] + [J_3, a]^\dagger [J_3, a] & [[J_-, a], [J_3, a]] \\ -[[J_+, a], [J_3, a]] & [J_-, a]^\dagger [J_-, a] + [J_3, a]^\dagger [J_3, a] \end{bmatrix} \right\| \\ &\geq \frac{1}{r^2} \sup_{\substack{|\psi_1\rangle \in \mathcal{H} \\ \|\psi_1\|=1}} \langle \psi_1 | [J_+, a]^\dagger [J_+, a] + [J_3, a]^\dagger [J_3, a] | \psi_1 \rangle \left(\psi = \begin{pmatrix} |\psi_1\rangle \\ 0 \end{pmatrix} \right) \\ &\geq \frac{1}{r^2} \sup_{\substack{|\psi_1\rangle \in \mathcal{H}_c \\ |\psi_1\rangle \langle \psi_1| = 1}} \langle \psi_1 | [J_+, a]^\dagger [J_+, a] | \psi_1 \rangle + \frac{1}{r^2} \sup_{\substack{|\psi_1\rangle \in \mathcal{H}_c \\ |\psi_1\rangle \langle \psi_1| = 1}} \langle \psi_1 | [J_3, a]^\dagger [J_3, a] | \psi_1 \rangle \\ &\geq \| [J_+, a] \|_{\text{op}}^2 + \| [J_3, a] \|_{\text{op}}^2. \end{aligned} \quad (241)$$

Therefore we get

$$\frac{1}{r} \| [J_+, a] \|_{\text{op}} \leq \| [\mathcal{D}, \pi(a)] \|_{\text{op}} \quad \frac{1}{r} \| [J_3, a] \|_{\text{op}} \leq \| [\mathcal{D}, \pi(a)] \|_{\text{op}}. \quad (242)$$

For $a = a^\dagger \in \mathcal{A}$, $[J_+, a]^\dagger = -[J_-, a]$ and using $\|A\|_{\text{op}} = \|A^\dagger\|_{\text{op}}$ as shown above, we get

$$\frac{1}{r} \| [J_-, a] \|_{\text{op}} \leq \| [\mathcal{D}, \pi(a)] \|_{\text{op}}. \quad (243)$$

For $a = a^\dagger \in B$ i.e $\|[\mathcal{D}, \pi(a)]\|_{\text{op}} \leq 1$ it thus follows that

$$\|[J_+, a]\|_{\text{op}} \leq r \quad ; \quad \|[J_-, a]\|_{\text{op}} \leq r. \quad (244)$$

□

References

- [1] Scholtz F G and Chakraborty B 2013 *J. Phys. A: Math. Theor.* **46**, 085204.
- [2] Martinetti P and Tomassini L 2013 *Commun. Math. Phys.* **323**, 107-141.
- [3] Doplicher S, Fredenhagen K, and Roberts J E 1995 *Commun. Math. Phys.* **172**, 187.
- [4] Yendrembam C D, Prajapat S, Mukhopadhyay A K, Chakraborty B and Scholtz F G 2015 *J. Math. Phys.*, **56**, 041707.
- [5] Connes A 1994 *Non-Commutative Geometry* (New York: Academic).
- [6] Van den Dungen K and van Suijlekom W D 2012 *Rev. Math. Phys.* **24** 1230004.
- [7] Cagnache E, D'Andrea F, Martinetti P and Wallet J-C 2011 *J. Geom. Phys.* **61** 1881.
- [8] Martinetti P, Mercati F and Tomassini L 2012 *Rev. Math. Phys.* **24** 1250010.
- [9] Latremoliere F 2012 *Quantum locally compact metric spaces* arXiv:1208.2398 [math-ph];
Wallet J-C 2012 *Rev. Math. Phys.* **24** 1250027.
- [10] A M Perelomov “Generalized coherent states and some of their applications” *Sov.Phys.Usp.* **20** 9 (1977).
- [11] H. Grosse , P. Prešnajder, “The construction of Non-commutative manifolds using coherent states” *Lett. in Math. Phys.* **28** 239-250 ,1993.
- [12] D'Andrea F, Lizzi F, and Varilly J C 2013 *Lett. Math. Phys.* **103** 183.
- [13] Scholtz F G, Chakraborty B, Govaerts J and Vaidya S 2007 *J. Phys. A: Math. Theor.* **40** 14581.
- [14] Scholtz F G, Gouba L, Hafver A and Rohwer C M 2009 *J. Phys. A: Math. Theor.* **42** 175303.
- [15] Galluccio S, Lizzi F and Vitale P 2008 *Phys. Rev. D* **78** 085007;
Balachandran A P and Martone M 2009 *Mod. Phys. Lett. A* **24** 1721;
Balachandran A P, Ibort A, Marmo G and Martone M 2010 *Phys. Rev. D* **81** 085017.
- [16] Provost J P and Vallee G 1980 *Commun. Math. Phys.* **76** 289.
- [17] Ashtekar A and Schilling T A 1997 Geometrical formulation of quantum mechanics arXiv:9706069 [gr-qc].
- [18] D'Andrea F 2015 Pythagoras Theorem in Noncommutative Geometry arXiv: 1507.08773 [math-ph].
- [19] Basu P, Chakraborty B and Scholtz F G 2011 *J. Phys. A: Math. Theor.* **44** 285204.
- [20] Connes A 1995 *J. Math. Phys.* **36** 6194.
- [21] Bratelli O and Robinson D W 1987 *Operator Algebras and Quantum Statistical Mechanics* vol 1 2nd edn (Berlin: Springer) p 76.
- [22] Iochum B, Krajewski T and Martinetti P 2001 *J. Geom. Phys.* **37** 100-125.
- [23] Conway J B 1990 *A Course in Functional Analysis* 2nd edn (New York: Springer) p 32.
- [24] Rohwer C M and Scholtz F G 2012 Additional degrees of freedom associated with position measurements in non-commutative quantum mechanics arXiv:1206.1242 [hep-th].